

# Instrumentation and control selection for the 12 GeV Hall B magnets at Jefferson Lab

Probir K Ghoshal<sup>1</sup> , Ramakrishna Bachimanchi<sup>2</sup>, Ruben J Fair<sup>1</sup>, David Kashy<sup>1</sup>, Renuka Rajput-Ghoshal<sup>1</sup>, John Hogan<sup>3</sup>, Nicholas Sandoval<sup>1</sup> and Glenn Young<sup>4</sup>

<sup>1</sup> Experimental Nuclear Physics Division, Thomas Jefferson National Accelerator Facility, Newport News, VA 23606, United States of America

<sup>2</sup> Engineering Division, Thomas Jefferson National Accelerator Facility, Newport News, VA 23606, United States of America

<sup>3</sup> LCLS-II Division, Thomas Jefferson National Accelerator Facility, Newport News, VA 23606, United States of America

<sup>4</sup> 12 GeV Project Division, Thomas Jefferson National Accelerator Facility, Newport News, VA 23606, United States of America

E-mail: [ghoshal@jlab.org](mailto:ghoshal@jlab.org)

Received 28 February 2018, revised 2 July 2018

Accepted for publication 10 July 2018

Published 8 August 2018



## Abstract

As part of the Jefferson Laboratory (JLab) 12 GeV accelerator upgrade, the experimental physics Hall B detector system requires two superconducting magnets—a torus and a solenoid. The specifications required maximum space for the detectors which led to the choice of conduction cooling for each magnet. The torus consists of six trapezoidal ‘race-track’-type coils connected in series with an operating current of 3770 A. The solenoid is an actively shielded 5 Tesla magnet consisting of five coils connected in series operating at 2416 A. Within the hall the two magnets are located in close proximity to each other and are surrounded by particle detectors. We describe the philosophy behind the instrumentation selection and control design that accounts for this proximity and other challenging working conditions. We describe the choice of sensor technologies, as well as the control and data acquisition methods. The magnet power and cryogenic control sub-systems are implemented using Allen Bradley Control-Logix 1756-L72 programmable logic controllers (PLCs). Sensor instrumentation readbacks are routed into the PLC via National Instruments cRIO hardware (field programmable gate arrays or FPGA/RT application) using a JLab-designed FPGA-based multi-sensor-excitation-chassis. Configuration, monitoring, and alarm handlers for the magnet systems are provided via an experimental physics instrumentation and control system interface. Failure modes and effects analysis and the requirement to monitor critical parameters during operation guided the selection of instrumentation and associated hardware. The design of the quench protection and voltage tap sub-systems was driven by the anticipated level of voltages developed during a magnet quench. The primary-hardwired quench detection and protection sub-system together with the secondary PLC based protection sub-system is also discussed. The successful commissioning and subsequent performance of these magnets demonstrates the robustness of the design and implementation approach that was adopted by the JLab team and serves as an excellent ‘how to’ guide for future projects of this size and complexity.

Keywords: conduction-cooled, superconducting magnet, magnetic field, instrumentation, protection, 12 GeV

(Some figures may appear in colour only in the online journal)

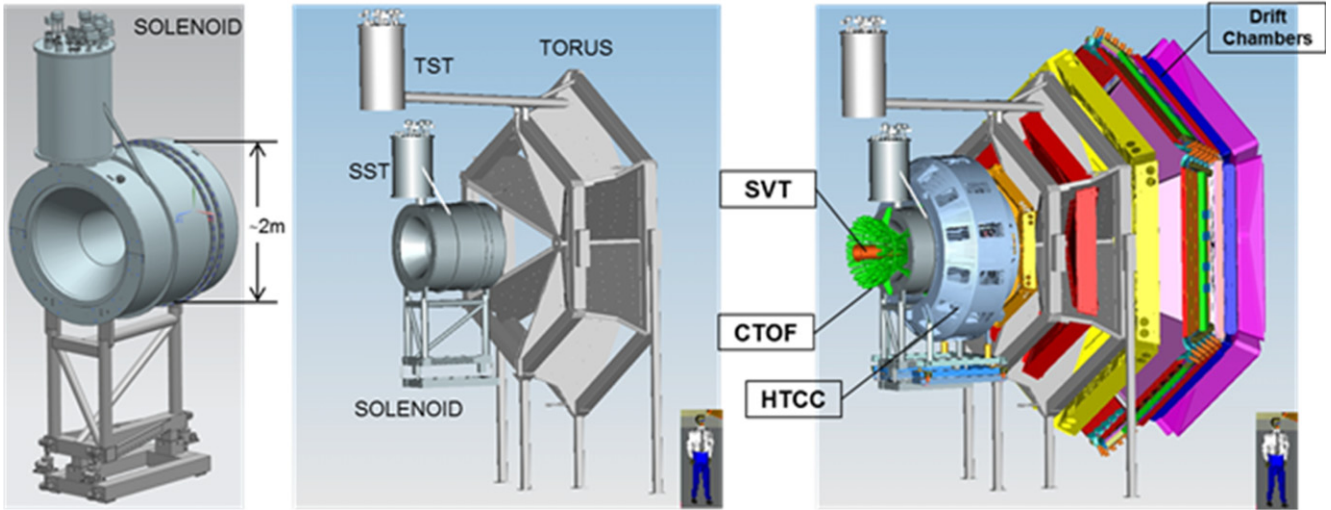


**Figure 1.** Computer-aided design (CAD) representation of solenoid and torus magnets as installed in Hall B, with physics detectors. The electron beam travels from left (upstream) to right (downstream) in the pictures.

## 1. Introduction

As part of the Jefferson Lab (JLab) 12 GeV accelerator upgrade, Hall B requires two superconducting magnets for the CEBAF large acceptance spectrometer (CLAS12) experiment [1, 2]. The magnets comprise a six-coil torus and an actively shielded 5 T large bore solenoid both of which are conduction-cooled with helium. The superconducting solenoid and torus magnets are installed in the hall together with all the required particle detectors. The torus magnet is at the downstream end of the solenoid magnet around the beam line as shown in figure 1. The solenoid magnet was designed and fabricated by Everson Tesla Inc., USA. The torus magnet was designed and assembled at JLab while the coils were fabricated at the Fermi National Accelerator Laboratory, USA [3]. The overall protection system design, instrumentation and control for both the torus and solenoid have been engineered by JLab. The behavior of the magnets is markedly different from that of more conventional bath-cooled superconducting magnets. A failure modes and effects analysis (FMEA) process (required as part of the JLab Risk Assessment and Mitigation (RAM) program) was utilized to ensure the robustness and safety of both magnet designs [4].

The overall 12 GeV project included upgrading the experimental equipment in three out of four halls—i.e. Halls B, C, and D which was a newly constructed hall. The solenoid magnet within Hall D was a re-purposed magnet from Stanford and was re-built, installed and commissioned before the magnets in Halls B and C had even begun construction and therefore the equipment was tailored specifically to its magnet. Hence, a decision was made at the beginning of the upgrade for Halls B and C that, wherever possible, similar equipment should be used in both the halls to allow ease of operation, and future support and maintenance. As an example, the superconducting magnet power supplies for Hall C had been purchased early—therefore, in order to keep costs down, power supplies of the same voltage and current ratings (as for the Hall C magnets) were

ordered for the new magnets in Hall B, with the understanding that we would not need to utilize the full 4000 A current rating. This decision allowed the power supply vendor to simply reissue the same drawings for a re-manufacture of these supplies without the need for any additional design work—the only difference being in the size and rating of the external dump resistors. Similar decisions were made with regards to the programmable logic controllers (PLCs)—which also made sourcing of individual PLC modules more straightforward and cost-effective.

As the Hall B torus and solenoid magnets were unique designs, when compared to the other superconducting magnets at the laboratory, the JLab team upgraded the instrumentation system to include more sensors in more locations and also included redundant sensors. Similarly, the overall control system was developed to provide a level of redundancy which included both networked and local devices—again a somewhat more involved approach when compared to the other halls.

## 2. System design

The torus magnet has six independent coil cold masses (CCM) with a helium re-cooler in between each pair of CCMs which also houses the conduction-cooled splices (figure 2). All six coils share a common vacuum space with two vacuum pumping systems being operated continuously—one at the top of the torus and the other located at the bottom.

The solenoid magnet has five coils in series, four main coils and one long thin shield coil as shown in figure 3. The two main coils (Coils #3 and #4) are wound into pockets on the main coil bobbin while the other two main coils (Coils #1 and #2) are shrink-fit into this bobbin. The shield coil is wound onto its own bobbin. These two bobbins are connected by four cross members. All coils are supported via eight radial and eight axial supports. Coils are conduction-cooled and Cu cooling sheets were potted with the coils for thermal

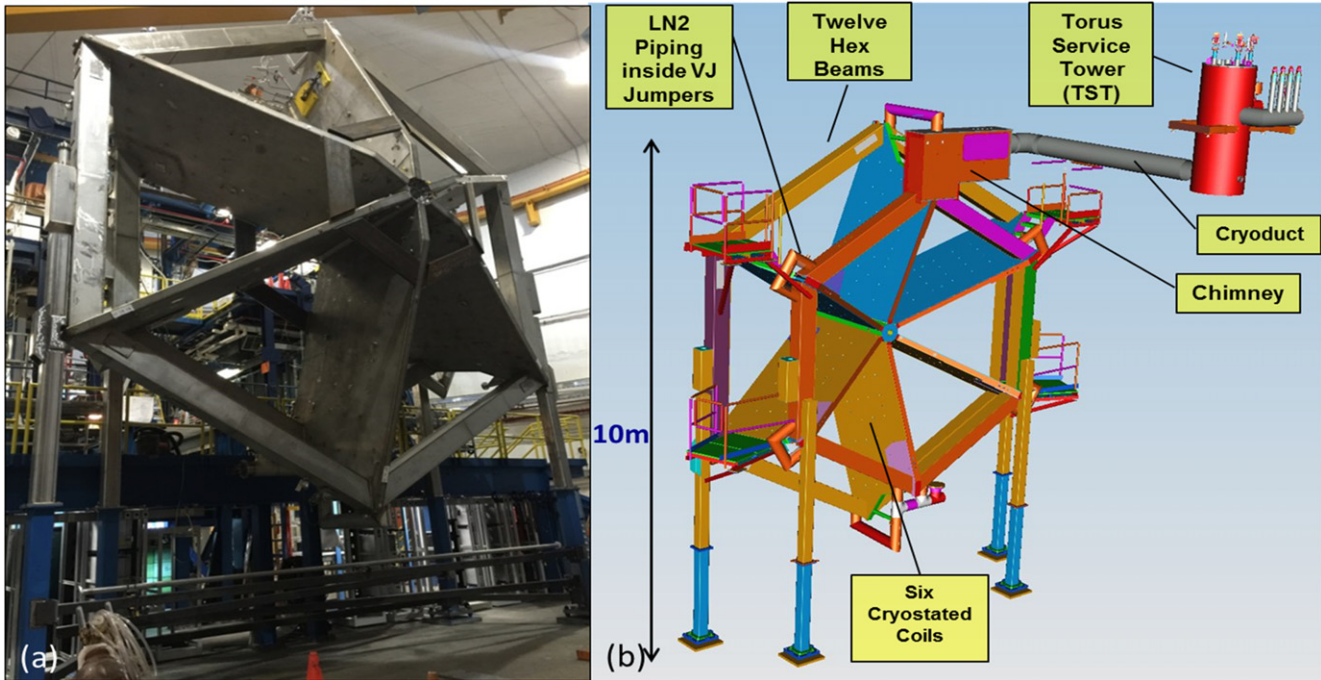


**Figure 2.** (a) Torus magnet installed (before detectors are installed in and around it), looking upstream, (b) CAD model of the torus magnet indicating the main system components, looking downstream.

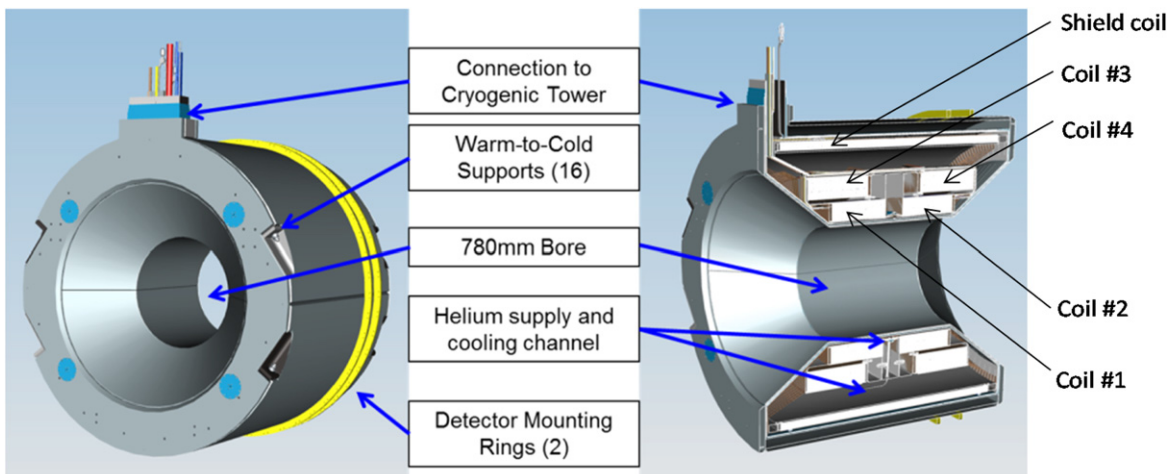


**Figure 3.** Solenoid magnet design.

communication with an annular helium cooling channel. The solenoid does not have a need for helium re-coolers in between the coils. All coils are located within the same vacuum space which is pumped on continuously by one vacuum pumping system.

Each magnet has its own cryogenic service tower which is fed via a common cryogenic distribution box. The various monitoring, control, protection, power, vacuum and cooling sub-systems (in figure 4) are largely similar for both magnets and are separate systems, although a cryogenic ‘event’ in one magnet can affect the other magnet and vice versa as both magnets share the same distribution box.

Being conduction-cooled magnets with a limited volume of liquid helium within each magnet, it is even more important to keep all heat loads to a minimum.

Both magnets are also required to operate in either polarity—i.e. clockwise or anticlockwise (positive) field direction for the torus and downstream (positive) or upstream field direction for the solenoid.

All pressure related components are required to comply with all the relevant American Society of Mechanical Engineers pressure vessel and piping codes.

Depending on where instrumentation was mounted on the magnet, all selected sensors had to be compatible with cryogenic temperatures and magnetic fields with regards to reliability and reproducibility of readouts with all detectors at its final locations.

The cycling of large currents in the superconducting magnets during ramp up and ramp down operations results in heat loads caused by eddy current effects and, together with

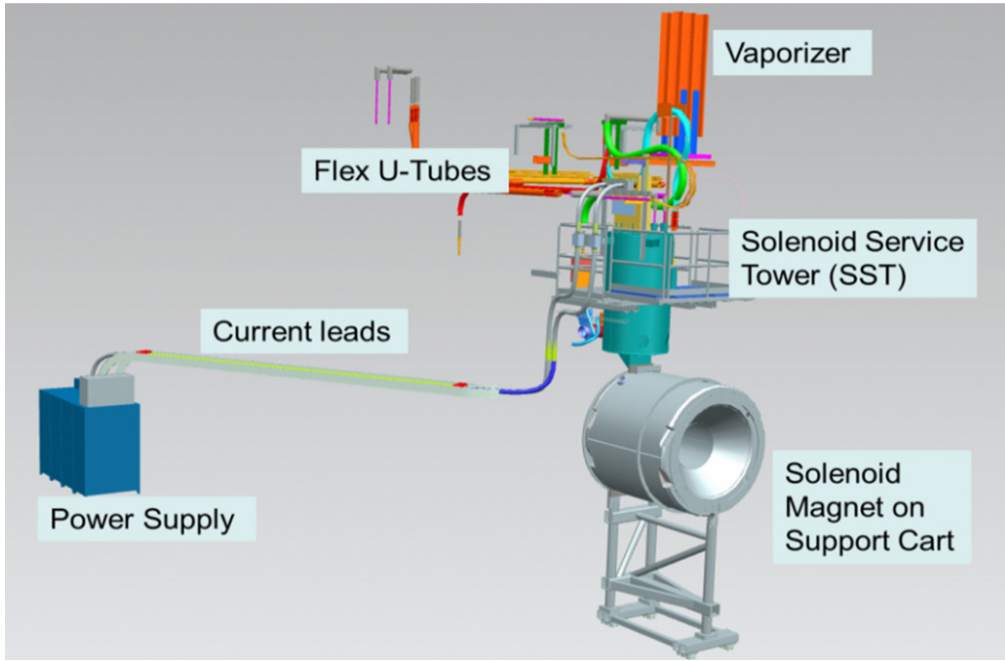


**Figure 4.** Solenoid magnet design indicating the main system components—view upstream of beam line.

the level of ambient noise within the experimental hall, also guided some of the instrument choices. The risk analysis also identified the various forces that arise during operation of the torus and solenoid magnets, namely eddy current forces, Lorentz forces, thermal loading [5, 6], and also the electromagnetic and cryogenic interaction between the torus and solenoid magnets [7]. For safe magnet operation, it is necessary to monitor and control all the following parameters: temperatures, pressures, pressure drops, liquid levels, mass flows, vacuum levels, voltages, strains, and loads. Extensive instrumentation was used to verify the design under various operating conditions during commissioning [8] and to allow flexible, reliable and safe control of all sub-systems by non-expert personnel post-commissioning.

Instrumentation was monitored using the following key elements:

- (a) JLab-designed sensor excitation electronics and National Instruments cRIO (slow data acquisition (DAQ)): magnet temperatures and strains;
- (b) National Instruments cRIO (fast DAQ): magnet-related voltages;
- (c) Cryo-Con (Cryogenics Control Systems Inc.) read out units: cryogenic system temperatures;
- (d) PLC: cryogenic system pressures, vacuum levels.

Monitoring and control of the entire system (including valves and flow indicators) was performed by Allan Bradley PLCs.

The magnet quench protection system (QPS) comprises primary and secondary quench protection sub-systems. Parallel path voltage taps (VTs) from multiple locations throughout the magnet (magnet coils, splices, bus-bars, leads, etc) feed both these sub-systems. The VTs feeding the

primary protection sub-system are hardwired directly from the magnet to the Danfysik quench detector (QD) units—i.e. with no electronics or any software manipulation in between.

The secondary quench protection sub-system is also fed from the same VT locations but this time the information is acquired by a fast DAQ, using a National Instruments cRIO device, and then routed to a PLC which performs summations and subtractions of various voltages to provide backup for the hardwired primary sub-system. A quench-induced voltage which exceeds pre-set voltage thresholds for a certain time period will trigger the primary system closely followed by the secondary system. The dump switch will then be opened to isolate the power supply from the magnet and the majority of the stored energy will be dissipated within an externally connected dump resistor.

The magnet diagnostic system (MDS) includes the control and the DAQ sub-system. The MDS is used to monitor and display the status of the magnets during cool down, warm-up and normal operation. The MDS also includes a hardwired interlock safety system which protects both the magnets in the event of any fault scenario including quenches [4].

The key torus and solenoid coil parameters are given in table 1.

The following sub-sections provide more detail on various aspects of magnet or component design and instrumentation selection.

### 2.1. Electrical

During a quench scenario, the maximum expected voltage across any coil is about 579 V for the torus and 718 V for the solenoid. This is calculated with the dump resistor in circuit

**Table 1.** Torus and solenoid key parameters.

Parameter	Unit	Torus	Solenoid
Peak operating current	A	3770	2416
Operating temperature	K	4.7	4.5
Coil peak field	T	3.58	6.56
Number of coils	—	6	5 (4 + 1 shield coil)
Total stored energy	MJ	14	17
Inductance of the magnet	H	2.0	5.89
Dump resistance	$\Omega$	0.124	0.20

based on the Wilson model [9]. The presence of this high voltage on the pins of the multi-pin connectors for the VTs necessitated potting the vacuum-side of the connectors with epoxy (Stycast 2850FT Blue with Catalyst 9) to increase the electrical tracking distance to ground [10]. A typical vacuum feedthrough is shown in figure 5, before and after potting. After potting each feedthrough was also tested on the bench, in air and in helium gas at standard temperature and pressure. An extract from a test report for three of the feedthroughs is illustrated in table 2.

Each voltage tap from the magnet also incorporated an in-line resistor to limit any potential current flow to less than 5 mA in order to satisfy equipment safety requirements. Additional precautions were also taken to ensure that personnel could never be exposed to high voltages during any potential fault scenario.

## 2.2. Mechanical

**Torus**—The entire torus magnet cold mass is supported by three-axial ( $Z$ ) supports (in the beam direction), four-vertical ( $Y$ ) supports which support the 25 ton gravity load [2, 11], two-lateral out-of-plane supports (OOPS) at the central hub, and 24-coil OOPS (four per coil). Multiple load cases were studied to understand the structural integrity of the magnet under electromagnetic, gravitational and thermal loads in the coils and the coil cases [5]. Two types of stresses in the coil and the coil cases were analyzed: primary stresses (namely Lorentz forces and gravity loads, including any normal or shear stress), and secondary stresses (e.g. thermal stress) which are self-limiting and limited to local yielding and distortions.

- (a) Cool down analysis suggests that the coils are preloaded (via compression) at room temperature and all stresses due to cool down are secondary stresses.
- (b) During normal operation, Lorentz forces are experienced and the stresses are both primary and secondary.
- (c) Current imbalance—Lorentz forces generate  $\sim 70$  kN out-of-plane load (assuming a 10% current imbalance or 110% gravity loading), and the forces resulting from an imperfect coil (due to alignment tolerances and potting inside the coil case) are  $\sim 7$  kN.
- (d) Quench fault analysis—Lorentz forces due to a quench resulting from a single coil to ground short, and 110% gravity loading results in  $\sim 129$  kN out-of plane load.

**Figure 5.** A ten-pin voltage tap feedthrough before and after potting.

The torus coils are supported between hex beams (upstream and downstream) and the hub and will normally experience only minimal deflection. The coil OOPS takes out the sag in the coil due to gravity and reacts with any out-of-plane forces (due to misalignments during installation) via the adjacent coil. The OOPS, epoxied to the bellows, maintains vacuum and allows the OOPS to move during cool down. A failure to balance coils when energized will cause the magnet to fast discharge as part of the safety protocol. Ideally all OOPS should experience zero force (when coils are balanced and energized) apart from the gravity loading depending on which coil is being considered.

The FMEA suggested that it was critical to monitor and control the out-of-plane forces supporting the coil. Analysis suggested that two load sensing devices per coil (one on each side face) would be sufficient to monitor the coil location within its vacuum jacket and loading when energized. Since this is a critical component and the fact that the mid-section of the coil might experience some force imbalance when energized, a second pair of redundant load sensing devices was also recommended.

Two options were explored, first using temperature compensated strain gauges, and second using load cells for the OOPS with the following key requirements:

- (a) Access at room temperature is required to replace any damaged load sensing device or if they required recalibration.
- (b) The selection of load sensing device was based on load capacity and it either had to be insensitive to magnetic field or was capable of being calibrated to work in a magnetic field.

Either load cells or individual strain gauge bridges would have likely done the job. However, individual strain gauge bridges were not a preferred option as once the gauges had been installed on the coil, access would be impossible without cutting into the vacuum jacket. Furthermore, cost-effective load cells with directly readable voltage outputs were readily available and this option was finally selected.

The final assembly includes a room temperature demountable load cell (calibrated for use in a magnetic field) connected to the DAQ to allow real-time monitoring of the out-of-plane forces on each coil.

**Table 2.** An extract of the test report of the feedthroughs after potting.

HALL B TORUS MAGNET				
Hi-Pot tests in air and in STP helium gas after potting of voltage tap feedthroughs				
Test engineers	R Fair, P Ghoshal			
Test date	11-December-15			
Vendor	Kurt J Lesker			
Part no.	IFDRG107013			
Description	F/T, 10-PIN, CIRC, DE, 1KV, 5 AMP/PIN, 2/75", UHV, W/O and F/T, 19-PIN, CIRC, DE, 1KV, 3 AMP/PIN, 2/75", UHV, W/O			
Minimum requirements	PIN-PIN PIN-GND	580 V 470 V		
Pass / fail criterion	Leakage current must be 0.5 micro-Amps or less			
FEEDTHROUGH #1 (10 pin)				
STP AIR		STP HELIUM		
PIN-PIN	PIN-GND	PIN-PIN	PIN-GND	
Voltage (V)	Leakage current (micro-A)	Leakage current (micro-A)	Leakage current (micro-A)	Leakage current (micro-A)
25	0.3	0.4	0.2	0.1
50	0.3	0.3	0.2	0.2
100	0.3	0.2	0.2	0.2
250	0.3	0.2	0.2	0.2
400	0.3	0.3	0.1	0.2
500	0.3	0.3	0.2	0.2
520			0.2	0.2
540			0.2	0.2
560			0.2	0.2
580			0.3	0.2
600			0.3	
620			0.2	
640			0.2	
660			0.3	
680			0.2	
700	0.3	0.2		
750	0.3	0.3		
800	0.4	0.3		
999	0.4	0.3		
SAFETY FACTOR	1.7	2.1	1.2	1.2
VERDICT	PASSED	PASSED	PASSED	PASSED
FEEDTHROUGH #2 (10 pin)				
STP AIR		STP HELIUM		
PIN-PIN	PIN-GND	PIN-PIN	PIN-GND	
Voltage (V)	Leakage current (micro-A)	Leakage current (micro-A)	Leakage current (micro-A)	Leakage current (micro-A)
25	0.3	0.4	0.2	0.2
50	0.2	0.3	0.1	0.1
100	0.4	0.2	0.2	0.2
250	0.2	0.2	0.2	0.2
400	0.2	0.2	0.2	0.2
500	0.3	0.2	0.3	0.1
520			0.1	0.3
540			0.2	0.2
560			0.2	0.2
580			0.2	0.2
600			0.2	
620			0.3	
640			0.2	
660			0.2	
680			0.2	
700	0.3	0.1		
750	0.3	0.3		
800	0.4	0.3		
999	0.3	0.3		
SAFETY FACTOR	1.7	2.1	1.2	1.2
VERDICT	PASSED	PASSED	PASSED	PASSED
FEEDTHROUGH #3 (10 pin)				
STP AIR		STP HELIUM		
PIN-PIN	PIN-GND	PIN-PIN	PIN-GND	
Voltage (V)	Leakage current (micro-A)	Leakage current (micro-A)	Leakage current (micro-A)	Leakage current (micro-A)
25	0.3	0.3	0.1	0.3
50	0.2	0.2	0.1	0.4
100	0.2	0.2	0.1	0.2
250	0.3	0.2	0.2	0.2
400	0.3	0.2	0.2	0.3
500	0.2	0.3	0.2	0.2
520			0.2	
540			0.3	
560			0.2	
580			0.2	
600			0.2	
620			0.2	
640			0.2	
660			0.2	
680			0.5	
700	0.3	0.3		0.5
750	0.2	0.4		
800	0.3	0.4		
999	0.3	0.4		
SAFETY FACTOR	1.7	2.1	1.2	1.5
VERDICT	PASSED	PASSED	PASSED	PASSED

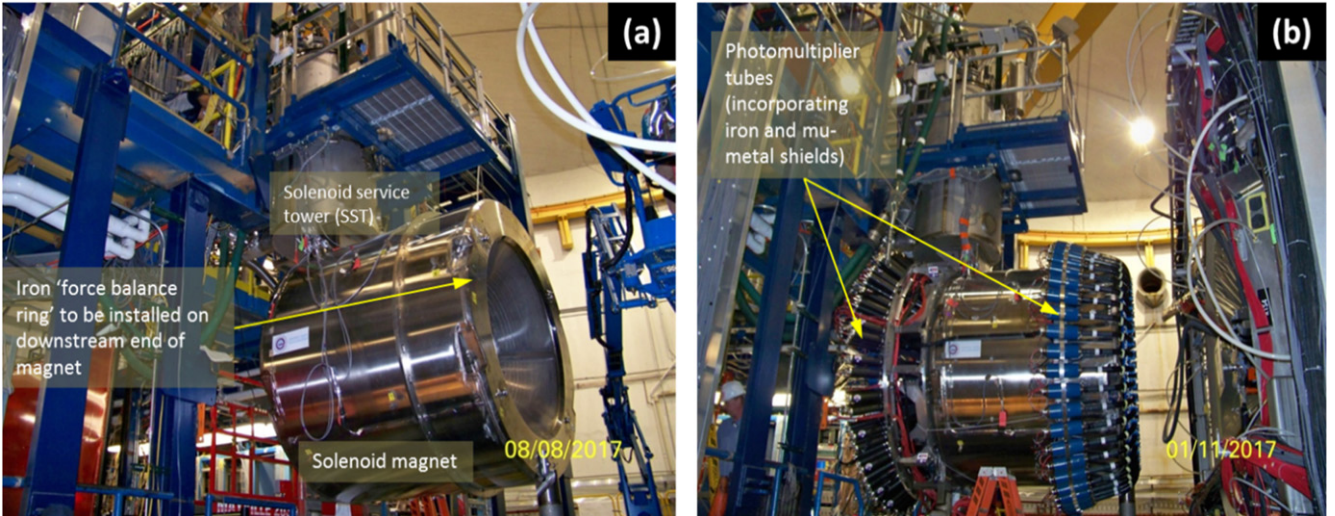


**Figure 6.** Solenoid magnet installed (a) before installation of physics detectors, and (b) with some physics detectors installed.

Strain gauges have however been used on some of the less risky components like the vertical supports and hex beams for the torus.

Since monitoring the temperature distribution across the coil was identified as being critical to limit thermal stress during cool down, a minimum of five Cernox™ sensors per coil was installed. Redundant Cernox sensors on the opposite side of each coil mirroring the first set of Cernox sensors were also installed.

**Solenoid**—The solenoid magnet cold mass is supported by eight axial ( $Z$ ) supports (in the beam direction), and eight radial supports. All supports were fitted with load cells which had been calibrated for use within a magnetic field and which, if necessary, could be accessed and replaced at room temperature—i.e. on the outside of the vacuum jacket. As for the torus, multiple load cases were studied to understand the structural integrity of the magnet under electromagnetic, gravitational and thermal loads in the coils. Two types of stresses in the coil are analyzed: primary stresses (namely Lorentz forces and gravity loads, including any normal stress or shear stress), and secondary stresses (e.g. thermal stress) which are self-limiting and limited to local yielding and distortions.

A detailed fault current and structural analysis was carried out for the solenoid magnet [12–17]. Studies of various fault conditions indicated that three critical scenarios can result, namely a very inhomogeneous field at the magnetic center of the magnet, a lower central field and a large stray field. Under normal operation with the solenoid and torus at full field (the solenoid being an actively shielded magnet) there is only minimal electromagnetic interaction between the two magnets. However, the studies showed that should the shield coil quench first, the stray field burst could (albeit briefly) increase axial forces between the two magnets which could lead to excessive stresses in the coil bobbins or suspension links [7]. It is therefore important to monitor the forces experienced by the solenoid's axial and radial supports (via load cells) during normal operation in order to initiate

either a fast discharge (via the dump resistor) or a controlled ramp down under certain fault conditions. In fact, these load cells also provide additional information on the movement of the cold mass during cool down and energization.

One of the detectors mounted in and around the solenoid incorporated photomultiplier tubes which had to be shielded from the stray field of the solenoid by the use of multiple passive shields, a combination of iron and Mu-metal (figure 6). As a result, the solenoid had to have an iron ring on one end to balance the axial forces produced by the photomultiplier shields during magnet energization, thus further reinforcing the need to continuously monitor the loading on the solenoid's axial supports.

### 2.3. Cryogenics

**Torus**—The 4 K cold mass (coils and hex beams) is shrouded within thermal shields which are actively cooled by liquid nitrogen that flows via the thermo-siphon effect. The magnet is held at the operating temperature by indirect cooling (conduction cooling) from a circuit of supercritical helium flowing in pipes, co-wound with the coils on their inner radius [11]. This supercritical helium circuit is re-cooled between each coil by a set of heat exchangers (re-coolers) located inside the hex beams that connect and support the coils. The splices that connect two adjacent coils are mounted directly on the heat exchanger and are cooled indirectly. Instrumentation with redundancy is provided to monitor and control the magnet cool down and steady state operation.

A simplified schematic of the cooling scheme [8] is shown in figure 7, and consists of three flow circuits as follows.

- The 1.3 atm. helium circuit from the torus service tower to the magnet hex beam re-coolers based on thermo-siphon flow provides re-cooling of the supercritical helium circuit between the coils to preserve the necessary operational temperature margin.

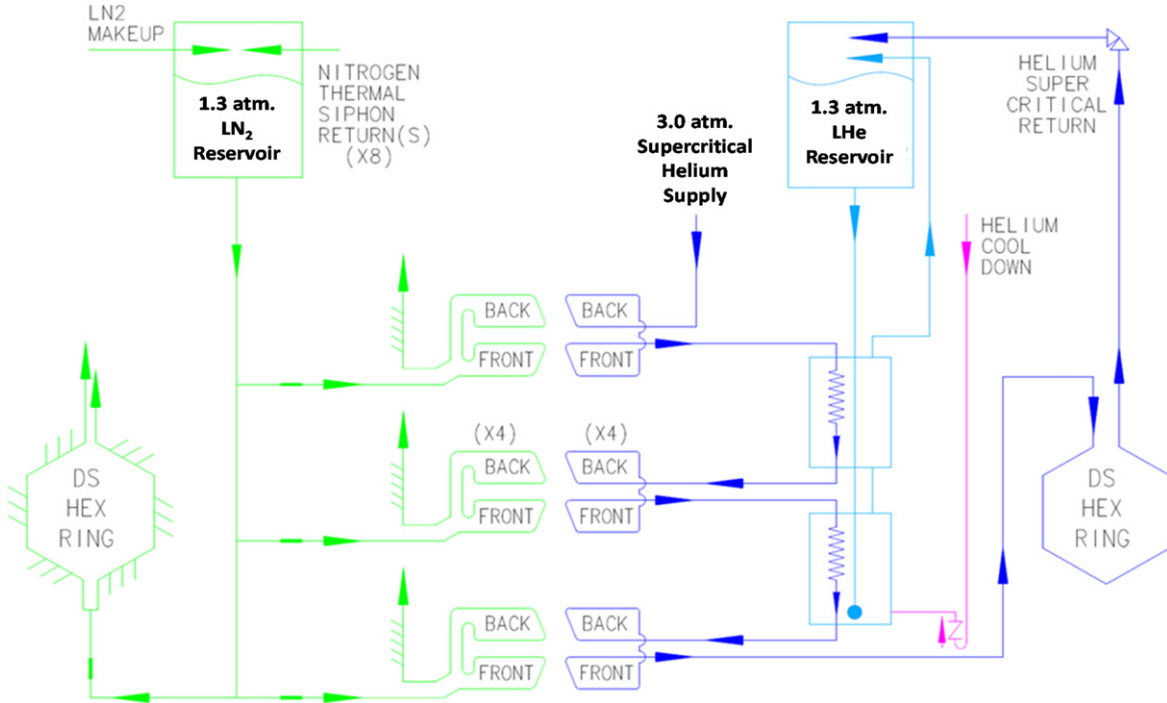


**Figure 7.** Simplified flow diagram of the Clas12 torus helium and nitrogen cooling circuits.

- (b) The supercritical 3.0 atm. helium circuit is a one-pass circuit through six coils and through the downstream hex beams and returns through the re-coolers in the upstream hex beam circuit.
- (c) The 1.3 atm. LN<sub>2</sub> circuit is also based on thermo-siphon flow with one feed and eight parallel branches (two feed-downstream hex beam shields; six feed coil shields and the upstream hex beam shields) to keep the shields at ~80 K. All are cooled by variable temperature gas from the distribution box to limit cool down stresses on the CCM and the shields.

**Solenoid**—The five-coil magnet is also conduction-cooled using a 4.5 K helium supply. Each epoxy-potted coil has copper cooling fingers and plates potted onto the surface of the coil. These cooling links are thermally connected to an annular helium channel. The liquid helium channel is situated between the coils center annulus along the inner diameter of the inner coils. The thermal shields are actively cooled by boiling helium gas from the magnet reservoir. The magnet is held at the operating temperature by indirect cooling (conduction cooling) via a thermo-siphon helium circuit from the magnet reservoir. Instrumentation with redundancy is provided to monitor and control the magnet cool down and steady state operation. The solenoid helium experimental physics instrumentation and control system (EPICS) control screen is shown in figure 8, consisting of two main flow circuits as follows:

- (a) 4.5 K, 3 atm helium from the JLab end station refrigerator is expanded (via the Joule–Thomson effect) within the lead reservoir at 1.3 atm. The lead reservoir feeds helium, both to the center annulus between coils

- (~1.2 l of volume) and the magnet reservoir. (Dark blue process lines in figure 8.)
- (b) Under normal operation, 1.2 atm. helium is fed from the magnet reservoir in the solenoid service tower (SST) to the bottom of the magnet’s annular cooling channel via a thermo-siphon action (light blue process lines in figure 8). The exhaust vapor exits through a split (parallel path) thermal shield circuit to keep the shield as a temperature lower than 80 K.

#### 2.4. Magnet field mapping

**Torus**—During commissioning of the torus magnet, the field mapping was carried out at different operating currents in order to establish the field profile and field error table. The magnetic field and deviation from the ideal model in the bore and between two coil sectors were measured. Results from the mapping identified two types of distortion within the magnetic field—shrinkage at low temperature and manufacturing and assembly tolerances (e.g. coils being shifted in the Z-direction, coils not being wound as tight as another, etc). This allowed engineers to adjust the electromagnetic model of the torus to match as-measured results. This matching is critical as the electromagnetic model and associated field map is subsequently used by the physics experimentalists to predict particle tracks.

- (a) Field mapping was performed along the Z-direction and at four locations between sectors at  $R = 0, 25$ , and  $50$  cm as shown in figure 9(a). Measurements were carried out at 3600 points: 6 (sectors)  $\times$  4 ( $X-Y$  position)  $\times$  3 (dimensions)  $\times$  50 (Z-direction).

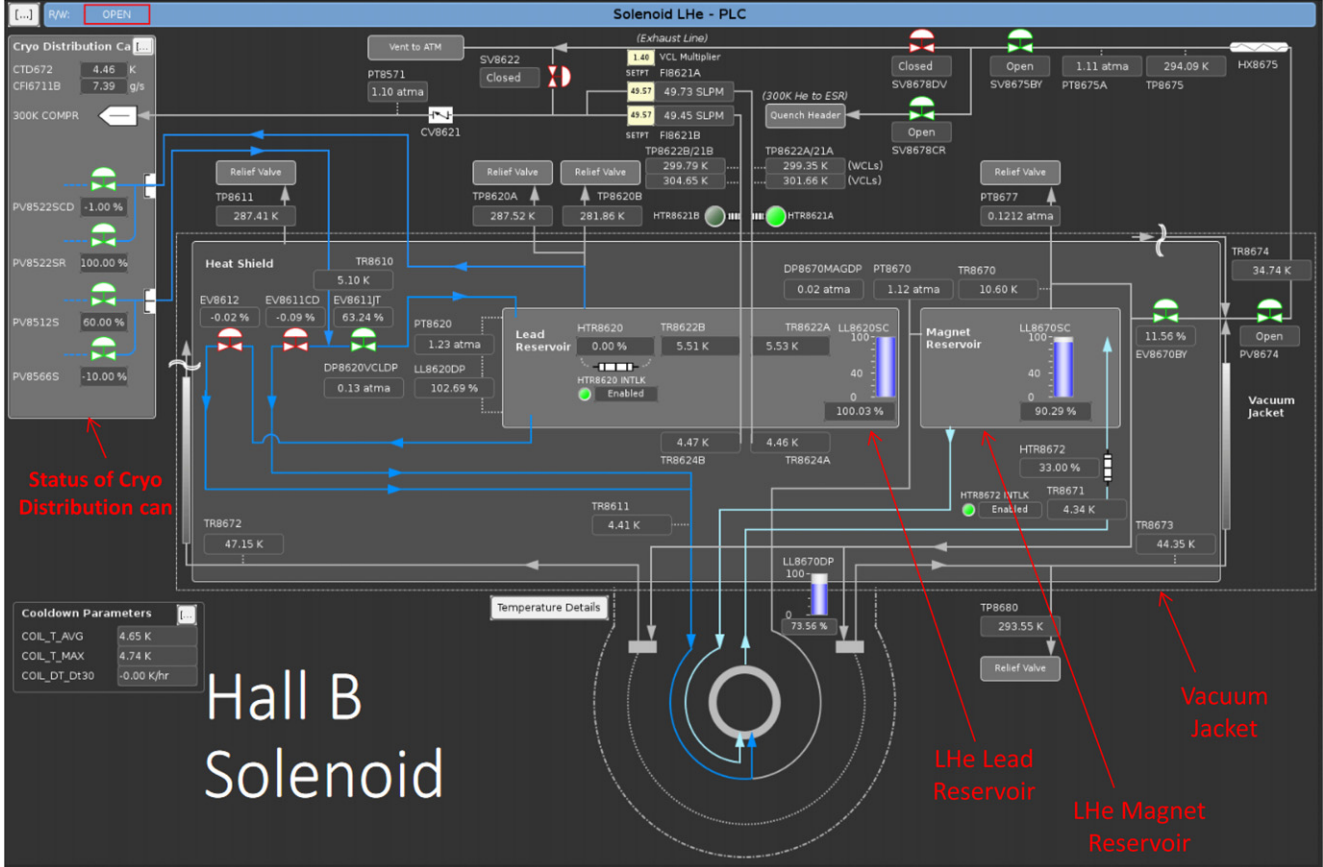


**Figure 8.** Clas12 Hall B EPICS control screen for solenoid helium process flow (cooling circuit for both magnet and thermal shield).

- (b) Positioning and alignment: the mapper prototype was built and tested prior to attachment to the magnet structure. The mapper consisted of a digital voltmeter, 2" diameter carbon tube referenced to survey points, three single-axis calibrated Hall probes (one for each of the X, Y and Z axes) positioned in a cylindrical block of Teflon® (as shown in figure 9(b)) spaced 5 cm apart in the Z-direction, and a control system (motion, data-recording, and interlocks).
- (c) Hall sensor for mapping: a commercially available Group 3 MPT-141 series transverse Hall probe with a DTM-151 teslameter was selected for the field measurement. The measurement accuracy at 25 °C with a shielded cable of L300 mm × ø6.5 mm is ± (0.01% of reading + 0.006% of full-scale) maximum. The Hall probes are temperature compensated and were also surveyed to a positional accuracy of 0.040 mm within the Hall probe holder.

The technique used earlier was experimented by Fry *et al* and Ikeda *et al* and was adopted for our measurement system [18, 19]. The Hall sensor mapper successfully demonstrated sensor placement, sensor movement, noise level, and data reproducibility better than 0.1% in the laboratory. The procedure required the accurate placement of four carbon fiber tubes within the magnet sectors. The sensor block is placed within a carbon tube in order to zero the Z-position of the

slide before the start of the Z-map for the particular location in question. The Z-map consisted of driving the sensor block in 5 cm steps along the Z-direction and pausing for 5 s for the Hall probes to settle before recording the probe data for each of the three sensors. The external fixture holds the 2" diameter carbon fiber tubes at precise X-Y positions and uses a linear stage drive to move the probes in the Z-direction as shown in figure 9(c). Real-time preliminary magnetic field analysis shows the sector-to-sector variation is better than ±0.5% (details are given in [20]).

**Solenoid**—During commissioning of the solenoid magnet, the field mapping was carried out at different operating currents in order to confirm the design specifications. The torus mapper was adapted for the field mapping of the solenoid magnet as shown in figure 10.

Field mapping was performed along the Z-direction at nine locations; one at the geometrical center of the magnet and at 8°–45° positions at a radius of 12.5 mm. The magnetic field was also measured along the z-axis at a 30 cm radius at a 60° angle. Measurements were carried out to establish the following:

- (a) to quantify the magnetic length of the solenoid;
- (b) to verify the high homogeneity region (25 mm diameter over 40 mm length) at the center of the magnet;
- (c) to measure the magnetic fringe fields at the specified detector locations.

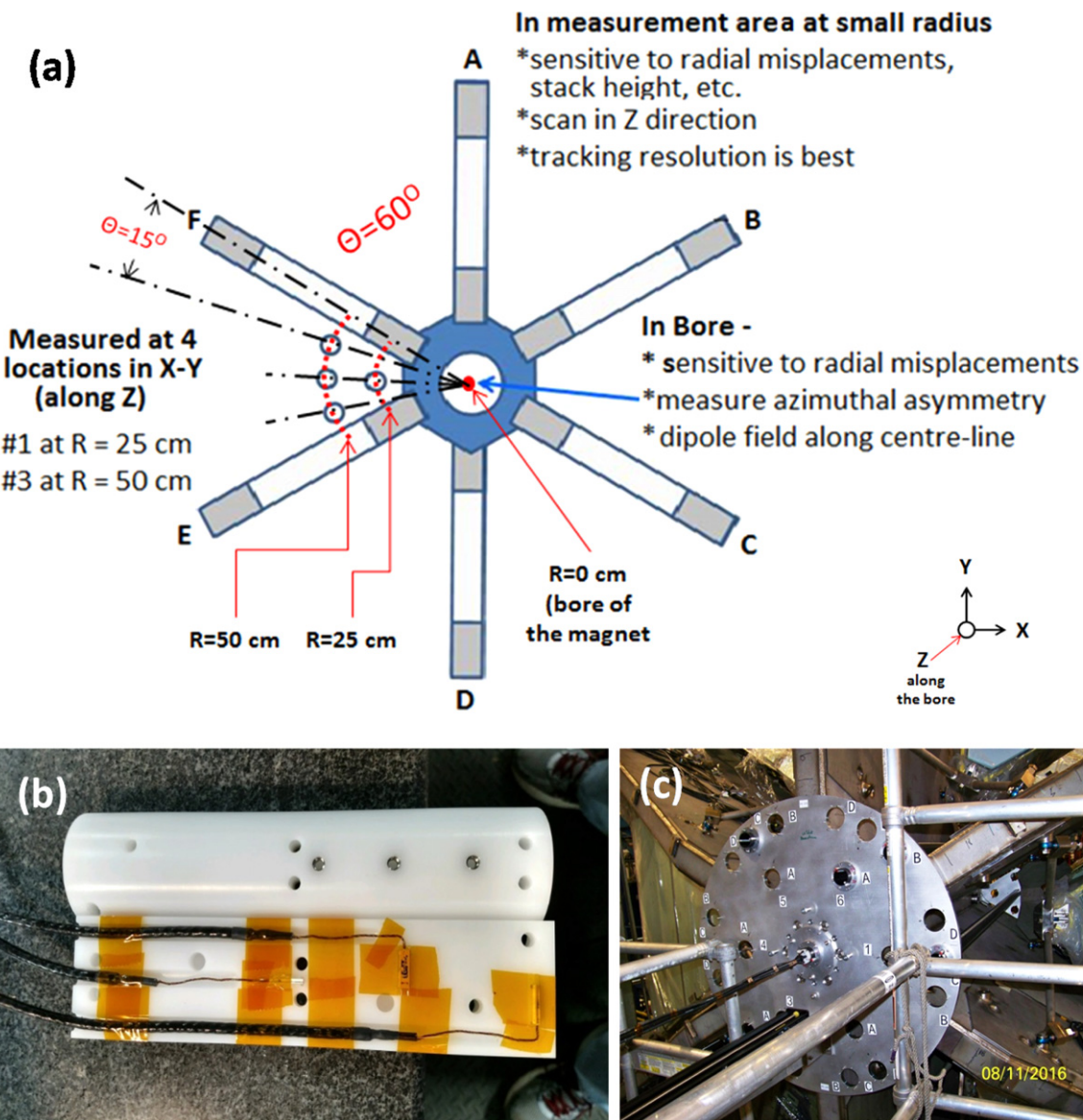


**Figure 9.** Measurement set up. (a) Typical magnetic field measurement locations for the torus magnet, (b) three single-axis Hall probes assembly located within a Delrin holder, (c) external fixture to hold 2" diameter carbon fiber tubes.

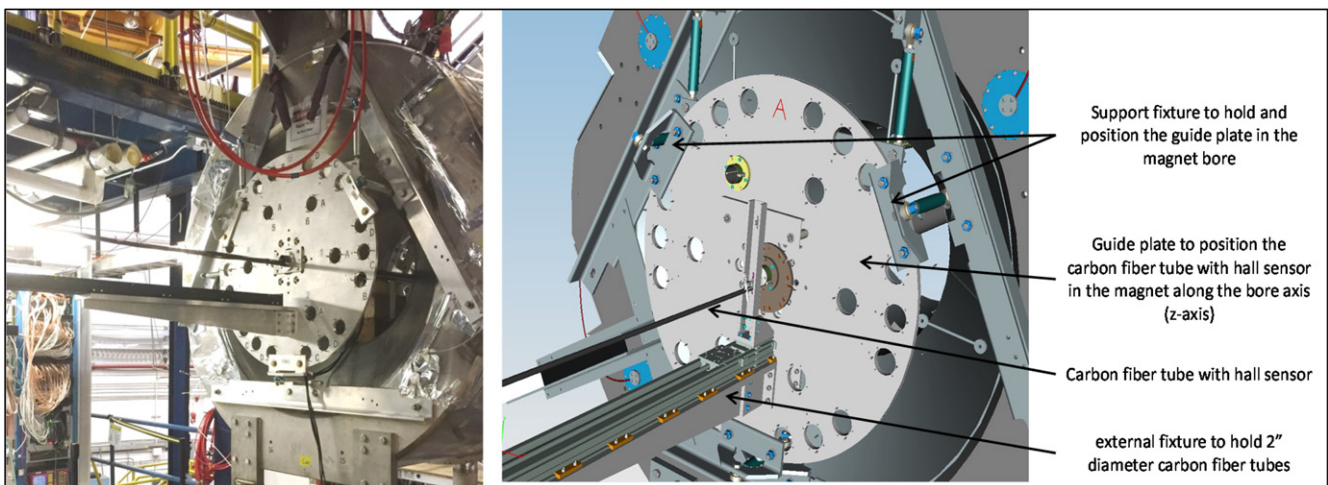


**Figure 10.** Typical arrangement for solenoid magnet field measurement along the bore and off-center locations.

**Table 3.** A brief summary of performance parameters.

Performance parameter	Broad specification	Actual measured
$B_0$	5 T	5.0 T
$L = B_0^{-1} \int B \cdot dl$ ( $B_0$ field at the center (0, 0, 0) of solenoid)	$L = 1\text{--}1.4$ m	1.41 m
Field at HTCC PMTs location	$B < 35$ Gauss for the four HTCC PMT locations	$B = 6\text{--}22$ Gauss
Field at TOF PMTs location	$B < 1200$ Gauss for the two TOF PMT locations	$B = 43\text{--}1041$ Gauss

High Threshold Cerenkov Counter (HTCC); photomultiplier tubes (PMTs); time of flight (TOF).

For verifying the field homogeneity of the magnet, measurements were taken only in the central part of the magnet at 10 mm intervals along the  $z$ -axis. The magnet length,  $L = B_0^{-1} \int B \cdot dl$  measured 1.41 m. The measured homogeneity,  $\Delta B/B_0$  in cylinder  $L = 40$  mm  $\times$   $\phi 25$  mm is better than 300 ppm and acceptable for meeting physics requirements. The measured magnetic fields at detector locations along with the magnetic length are summarized in table 3.

### 3. Risk mitigation strategy—sensors and technology

#### 3.1. Risk identification and mitigation

**3.1.1. General approach.** Taking the torus magnet first as an example, instrumentation sensors were installed on the CCM and on the thermal shield at key locations as directed by finite element analysis simulations. The thermo-mechanical instrumentation on the CCM is purely passive. Temperatures were acquired and checked at regular intervals, no interlocking of these signals was necessary. On the other hand, the load cells and the strain gauges on CCMs were interlocked to the magnet power supply (MPS) for a controlled run down via the PLC control system if the limits were exceeded. An FMEA [4] was carried out for each phase of the implementation: design, fabrication, installation, and commissioning. Identified risk items were then categorized, ranked, and subsequently mitigated.

The FMEA process was applied in two phases:

- (a) Phase 1: design and operation FMEA—addresses issues at the design stage, addresses magnet operation-related issues that lead into the design of the control and instrumentation system;
- (b) Phase 2: manufacturing, assembly and installation FMEA—coil manufacturing risks identified by JLab and Fermi Lab which provide input to the system assembly and installation processes and magnet operation FMEA.

All identified risks were then addressed in the order high  $\rightarrow$  medium  $\rightarrow$  low. A similar approach was used for the solenoid where failure modes were defined, categorized and addressed as shown in table 4.

Mitigations identified at the design stage continued through manufacturing, build and assembly, instrumentation and control, installation, commissioning and operation, as

summarized in table 4. For example, we identified 202 potential failure modes that could possibly exist after the solenoid magnet was built but before it was commissioned. A total of 195 of these failure modes were mitigated and seven were left in the medium category as they could only be mitigated during the commissioning phase of the magnet, as represented in figure 11. For example, one out of seven medium risks identified related to the SST with regards to a vapor cooled lead being improperly soldered when manufactured. A leak check after assembly and splice resistance can only be verified after the magnet was cooled and was being powered up.

**3.1.2. Mitigation of risk for torus coils.** The original plan called for only two of the torus coils to be tested at 4 K to prove the overall design and cooling efficacy. A test requirements document was sent out to five potential test facilities in the USA and Europe. For several of the test facilities, significant changes to their test infrastructure would have been necessary to meet the test requirements which would have led to a substantial increase in cost which the 12 GeV project could not absorb. Furthermore, several of the test facilities could not meet the required schedule for the delivery and test of the coils due to other work going on at their facility. The 12 GeV team was thus encouraged to explore alternatives. The team reviewed the pros and cons of a 4 K test versus an 80 K test and concluded that the ‘high’ and ‘medium’ category risks could be sufficiently mitigated by subjecting each torus coil to an 80 K test by flowing liquid nitrogen through each coil’s cooling tubes [21]. An extract from the team’s review report is provided in table 5.

The test included fully instrumenting each coil with temperature sensors and strain gauges, cooling it down close to 80 K, monitoring its steady state performance and comparing stress, strain and temperature results with those from finite element analyses and then warming up the coil. The cool down and warm-up processes were controlled to mimic cool down rates in the final magnet. Resistance, inductance and hi-pot tests were also carried out before, during and after the cool down test. Temperature distributions across the coil were scaled to 4 K conditions and confirmed that the conduction cooling method employed was working as designed. An extract from one of the coil test reports illustrating the scaled results is provided in table 6. All six coils plus one spare were cooled down to 80 K; all met the required thermal and electrical performance.

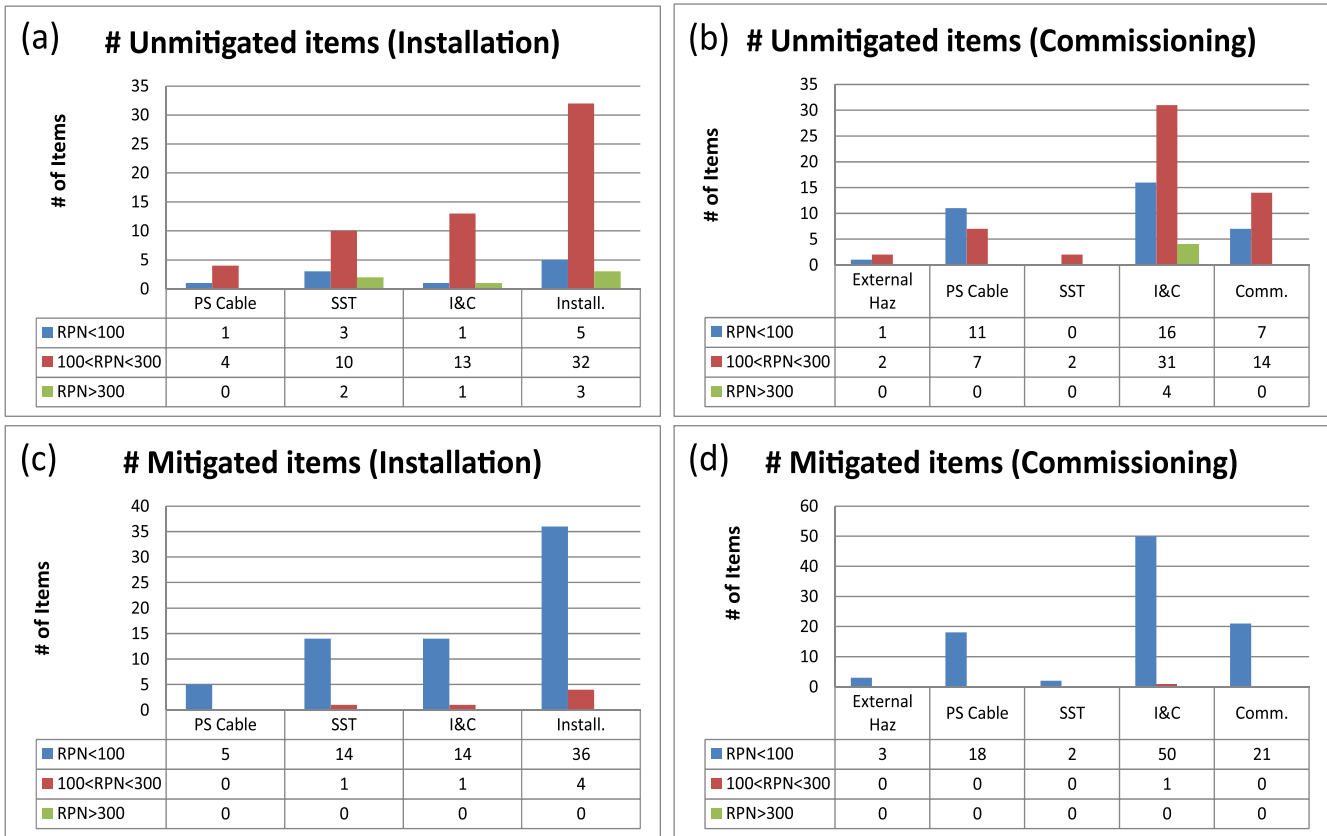


**Figure 11.** Total unmitigated and mitigated faults for the solenoid (a), (b) unmitigated fault prior to installation and commissioning, (c) and (d) mitigated during installation and commissioning.

**Table 4.** A brief summary of FMEA items for the solenoid prior to installation and commissioning (RPN = risk priority number).

Activity group	# Failure mode assigned		
External hazard	3		
Power supply and cable	25		
Solenoid service tower	22		
Instrumentation and control	91		
Installation	40		
RPN status	RPN < 100 (low)	100 ≤ RPN < 300 (medium)	RPN ≥ 300 (high)
Unmitigated U-RPN	63	128	11
Mitigated RPN	195	7	0

### 3.2. Sensor excitation and read out

The design of the sensor read back chassis was based on the requirements of the torus and solenoid instrumentation in terms of quantity and types. Commercially available read out boxes for every sensor are usually limited to a certain number of channels and the multi-functional capability of these devices usually means that these devices are expensive.

The motivation to accommodate all the sensor types (temperature, pressures, strains, loads, magnetic field—termed ‘slow data’) that would be used on both magnets together with a reduced set of functions, (i.e. to only meet the required control system needs of the magnets and no more), led to a JLab-designed and developed field programmable

gate arrays (FPGA)-based multi-sensor-excitation-low-voltage (MSELV or simply LV) chassis which sets the excitation current or voltage for a sensor and also provides read back. The data read back would then be routed to a NI-cRIO (the slow DAQ system) which would pass data to the PLC for control of the various sub-systems and interlocks, see figure 12.

Prior to designing the MSELV system, a smaller FPGA-based system developed earlier for superconducting radio-frequency cavities at JLab using ADCs and DACs, with some modification, was used for the 80 K test for the torus coils. With the experience gained from the 80 K test, a system was designed to suit the needs of both the torus and solenoid magnets. The MSELV chassis consists of different boards for

**Table 5.** An extract of the review report to evaluate risk and benefits of 4 K versus 80 K coil test.

Risk identified	Risk category	% of risk mitigated by performing 4 K test	% of risk mitigated by performing only 80 K test	Comments
1 Coil electrical insulation system fails	Medium	90	70	At 80 K we can only check insulation integrity as a function of thermal cycling, not as a function of stresses during energization or high voltages during quench. However note that even with a single coil test at 4 K, we still will not be testing at high quench energies or high voltages.
2 Coil cannot withstand mechanical stress due to cool down	Medium	100	100	At 80 K approximately 90% of thermal contraction will have occurred. Low risk that final 10% of contraction could cause movement and damage.
3 Coil cannot withstand mechanical stress due to energization	Low	90	0	Testing a single coil even at 4 K will not subject the coil to all the forces it would see in operation as part of a six-coil system. At 4 K we could run to higher than the operating current to increase stresses but would probably not want to do this.
4 Superconducting Super Collider conductor under-performs electromagnetically	Low	90	0	Limited current flow at 80 K will not provide any useful conductor performance information. Testing a single coil at 4 K will not allow for all the stresses and electromagnetic coupling present for a six-coil system.
5 Coil does not survive quench	Low	70	0	A single coil test at 4 K does not remove all the risk as the stored energy is low, current decay is very fast and there is no electromagnetic coupling with other coils.
6 Coil does not survive fast discharge	Low	100	0	With a single coil test at 4 K, the inductance is low, so we will have to artificially limit the fast discharge rate to match that predicted for a six-coil system.
7 Coil is not cooled effectively or cooling efficiency is poor	High	100	100	At 80 K approximately 90% of thermal contraction will have occurred. Low risk that final 10% of contraction could cause movement of cooling fins, soldered joints, insulation etc thereby affecting cooling.
8 Gauss/Amp of coil is incorrect	Low	100	90	We should be able to pass 10 A through the coil at 80 K and monitor the field.

**Table 6.** An extract from a 80 K coil test report.

	94 K test result front	94 K test result back	4 K scaled result front <sup>a</sup>	4 K scaled result back <sup>a</sup>	4 K ANSYS FEA <sup>b</sup>
Temperature difference at Hub (bore) (K)	8.73	5.07	0.36	0.21	0.251
Temperature difference at DS HEX (K)	11.39	12.67	0.46	0.52	0.834

<sup>a</sup> Estimated heat load from practice coil (CCM000) 80 K cool down ~500 W.

<sup>b</sup> ANSYS FEA assumed 13 W total heat load ( $2 \times 0.025"$  thick copper cooling sheets per coil side).

load cells, strain gauges, and temperature sensors and are based on the following.

- (a) Voltage-in and voltage-out board, used for strain gauges and load cells.
- (b) Voltage-in and current-out board with current output range between 1 and 5 mA, used for PT100 sensors.
- (c) Both the boards mentioned above employ the same printed-circuit-board (PCB) design with a few changes to the value of resistors. This approach simplifies the design, avoids designing two different boards and also makes future maintenance and upgrades easier.
- (d) Voltage-in voltage-out board along with a voltage-in current-out board with current output range of 200 nA–20  $\mu$ A is used for Cernox sensors and is based on the precision voltage to current converter application [22].

The circuit used for voltage read back used instrumentation amplifiers adopted from application notes on instrumentation amplifiers [22, 23]. All the designs are JLab designs based on the application of operational amplifiers, analog to digital converters (ADCs) and digital to analog converters (DACs). The DAC was used for different projects along with an operational amplifier to drive voltage or current. A commercial FPGA board [24] is used for communicating with the ADCs and DACs. This FPGA also communicates with the NI-cRIO via an RS232 interface. A PCB was designed by JLab to route signals to the different boards and RS232 communication with the NI-cRIO. All the boards went through a prototyping phase and extensive testing with various sensors in multiple combinations before going into production. This design is based on experience gained from extensive testing at 80 K and subsequently at 4.2 K during development at JLab. The torus required six chassis while the solenoid required two chassis.

Each chassis was designed to be able to address 56 channels. It uses a DAC (DAC8568 from Texas Instruments) to drive the input voltage to the operational amplifier as shown in figure 13. The output can be set to voltage or current by changing resistors, thus providing the flexibility to use the same modular design for all sensor types. Voltage is read back across the sensors using an instrumentation amplifier and an ADC (ADS1258 from Texas Instruments) for a true four-wire measurement in order to exclude the effect of lead wire resistance, as shown in figure 14.

The FPGA (Cyclone IV Nano-board from TERASIC) communicates with the ADC and DAC using a serial

peripheral interface protocol with the National Instrument's cRIO acting as a master, and communicates with the FPGA over RS232. This configuration sets the excitation voltage or current as required and reads the voltages back which subsequently get converted into engineering units.

### 3.3. Sensor selection

Any sensor selected for use either on the magnet itself or within the cryogenic sub-system had to be capable of operating reliably at cryogenic temperatures, in vacuum and in the presence of magnetic fields. These were key drivers and led to the selection of sensors as listed in table 7.

Additionally, the physical layout and the technologies utilized for the instrumentation were chosen so that there was redundancy in case of sensor failure.

The selection and placement of the sensors were therefore determined by ensuring:

- (a) periodic repeatability or symmetry (generic information made available from other identical sensors located in a symmetric location);
- (b) well proven technologies given the environmental conditions (4, 77 K, vacuum, and magnetic field).

Both the solenoid and torus magnets are instrumented extensively and readings are processed through the DAQ, to enable monitoring of the status of the magnets.

(a) *Strain gauges*—Cryogenic strain gauges and two part epoxy glues compatible with 4 K operation were selected and used throughout the 4 K environment. Cryogenic strain gauges are also used on the room temperature (or close to room temperature) portions of the vertical and axial supports for the torus magnet. The axial and vertical supports are stainless steel links connecting the cold mass to the vacuum jacket. The vertical units support the gravity load of the cold mass, while the axial supports react to loading in the beam direction (due to either manufacturing misalignments or seismic motion). The strain gauges (primary and redundant) are mounted to provide data for the principal direction of measurement. The read out data are averaged, but in case of one gauge failure, data will still be available for monitoring after making modifications to the read out program. These gauges are preassembled on the supports and calibrated before installation. The primary locations of strain gauges are

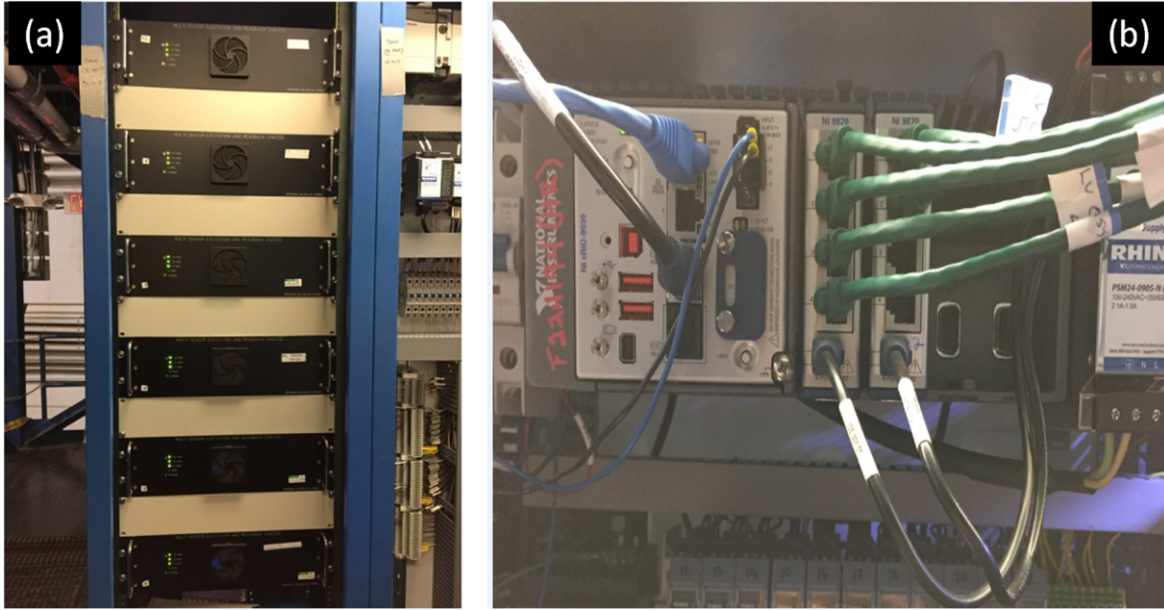


**Figure 12.** (a) The MSELV (six chassis for the torus magnet), and (b) slow DAQ NI-cRIO for slow data.

the CCM, hex beam, and supports. A bridge circuit chassis is added to the MSELV for strain gauge measurement. The bridge chassis employs a standard Wheatstone bridge with one of the bridge resistors as the strain gauge element while the remaining resistor elements are high tolerance resistors. The one opposite to the strain gauge has a potentiometer in order to balance the bridge circuit shown in figure 15. The system is passive and all required excitation voltages are from the LV chassis. The MSELV Chassis is an ADC which only allows positive voltage values, implying that the bridges have to be balanced high to ensure all the readbacks are positive [25].

- (b) *Temperature sensors*—The temperature monitoring of the magnet, magnet structures and interconnects covers the range 300–4 K. The required absolute precision on the measurement is expected to be <1% of the measured value at 4.2 K. Calibrated Cernox sensors from Lakeshore Ltd are used due to their low sensitivity in a magnetic field. A few silicon diode temperature sensors are also used within the cryo-service tower at 4.2 K where their exposure to magnetic fields is <0.1 T. For temperatures >70 K, a pair of PT100s (one redundant) embedded in an aluminum block are calibrated and mounted onto the segmented thermal shields to monitor the temperature distribution across the shield [6]. Excitation current for the PT100 is kept constant, but for Cernox sensors, it is varied (between 0.20 and 20  $\mu$ A) based on the criteria of voltage/power dissipation powered by the MSELV [26]. Again, this philosophy was applied to both magnets.
- (c) *Load cells*—The OOPS assembly includes a load cell (the Futek Model LCF450 was used on the torus magnet) connected to the DAQ/MSELV and enables easy mounting and replacement. These load cells offer

high accuracy and linearity within an operating temperature range of –60 °F to 200 °F. The loads cells were calibrated at JLab in magnetic fields up to 1.0 T under varying loads from 400 to 2000 lbs (using a conventional dipole magnet) before installation on the torus magnet.

- (d) *Hall probe sensors*—For the torus an axial hall sensor was mounted on each CCM's vacuum jacket (i.e. at room temperature). A constant 100 mA excitation current is provided to all six Hall sensors (via a separate current source) and voltage read out from each sensor by the MSELV. The solenoid uses three-axial hall sensors mounted on the outside of the vacuum jacket on the downstream end of the magnet.
- (e) *Level sensors*—Primarily two types of level sensors are employed for both the torus and solenoid, differential pressure, and superconducting capacitance probes. The capacitance probes are read out by an American Magnetics, Inc. Model 185 cryogen level monitor system (figure 16(b)) and the scaled output is fed directly to a PLC analog channel. For the case of the helium level, a locally employed interlock is fed directly to the power supply dump contactor as a secondary interlock. The differential pressure measurement is read out with a 3051 C Rosemount transmitter. The output is scaled and converted to a percent level in the PLC based on the physical dimensions of the tank.
- (f) *Wiring feedthroughs*—the wiring of the various sensors employed the following principles.
  1. Twisted pairs (shielded and grounded) to reduce electromagnetic noise pick-up.
  2. Constantan ( $Cu_{55}Ni_{45}$ ) wires are used in the form of ribbon cable on the 4.2 K mass and thermal shield, this is also thermally anchored to 4.2 and 80 K surfaces to minimize heat leak via conduction.

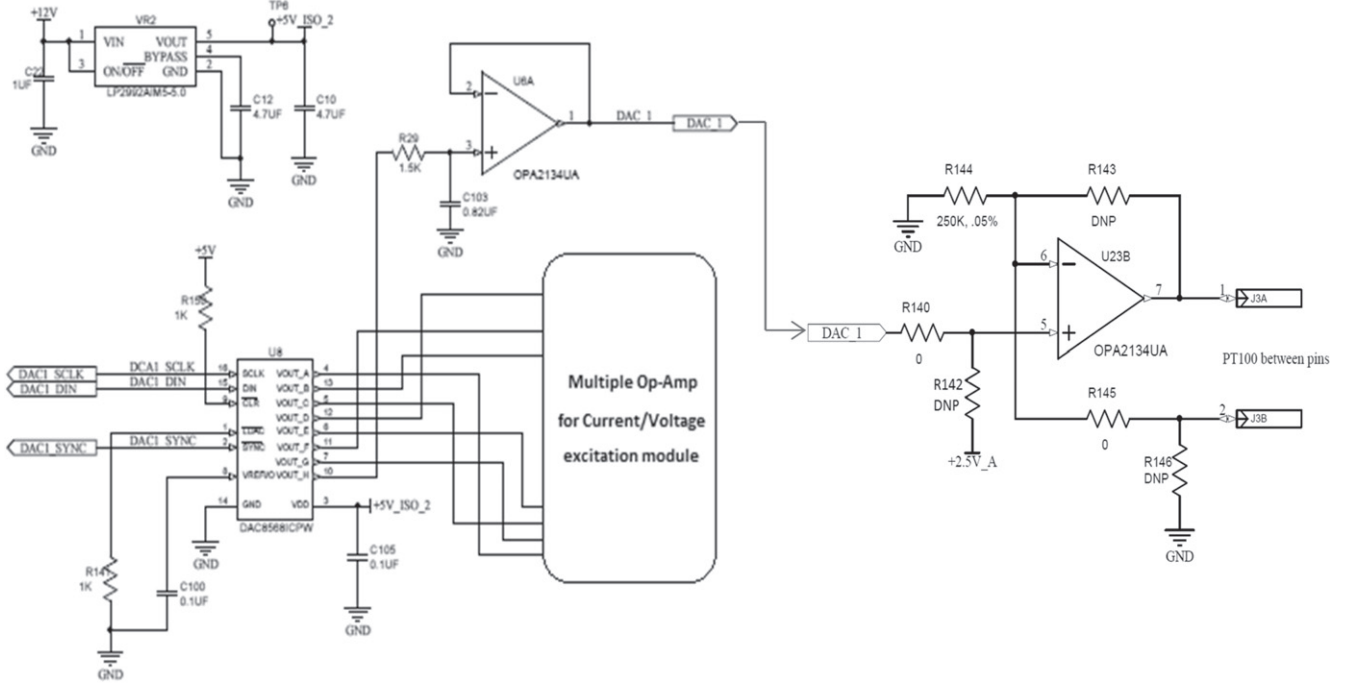


Figure 13. Typical current/voltage excitation circuit module.

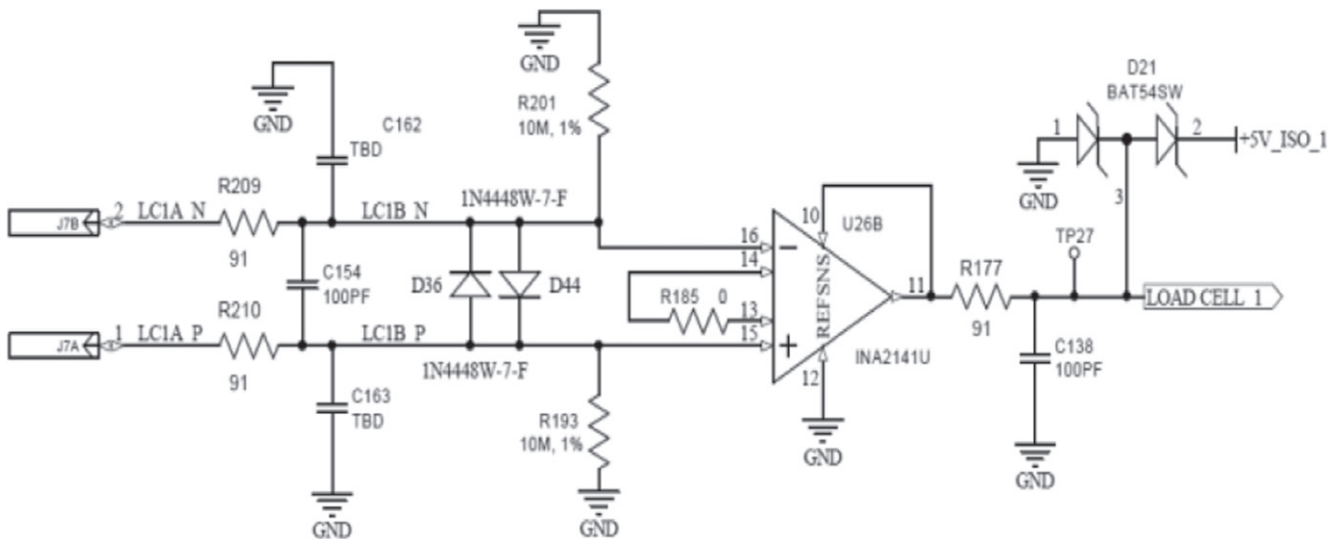


Figure 14. Typical modular channel read out circuit.

3. Two independent VTs are provided from the same location on the magnet, as suggested by the applied FMEA process.
  4. Voltage tap wires are 26 AWG multi stranded copper with 0.008" polyimide (Kapton®) film insulation. Sensor wiring and voltage tap wires were routed separately and terminated into separate vacuum feedthroughs featuring multi-pin bayonet-locking connectors [27] and qualified for a helium leak rate better than  $1 \times 10^{-9}$  mbar s $^{-1}$ .
- (a) *Control and instrumentation*—The majority of instruments are powered and read out via the LV chassis.

1. The MSELV sends the unscaled raw readouts to the NI-cRIO via individual RS232 ports. Each port is typically divided based on instrument type, temperature, load cell, etc. The NI-cRIO takes the raw data for each instrument and converts it to engineering units from specified calibration tables. This ‘slow’ data is sampled at 1 Hz.
2. The cRIO device puts scaled sensor readouts into arrays, based on instrument type, and sends these arrays to the PLC via ethernet.
3. The PLC then takes this data along with pre-specified routines (cool down, power up, etc) to

**Table 7.** Torus and solenoid magnet system sensors and voltage taps.  
**(A) TORUS Magnet System**

Measurement	Voltage		Temperature (4 K)		Temperature (77K)		Strain		Load cell		Hall sensor				
<b>Sensor/Wiring Type</b>	8mil Kapton insulated-multi-strand copper wire (pair)		Cernox™(1070) – 4 wire		Calibrated PT100 – 4 wire (Omega F2020-100-B)		Cryogenic series 350 Ω (CFLA-6-350) 4-wired/3-wired for measurement		LOAD CELL - FUTEK FSH02239 (2000 LBS), 4 wire, 300 K		Cryogenics hall generator (axial), HGCA-3020, 4 wire				
<b># sensors/wiring</b>	Magnet	23	Magnet	54	Thermal shield	60	Coil Cold Mass (CCM)	24	OOPS	26	Vacuum Vessel				
	Zero-Flux Current Transducer	2	Cooling Tube	12	Current - Leads	2+2	Axial sup	6	FMEA result	3 (Hub)					
	FMEA Result	1 (Power supply-One bus bar)	Splices	6+2	Axial sup	3	Vert sup	8							
	Line-GND/Dump Resistor	1	VCL in Cryostat	2+2	Vert sup	4	FMEA result	24 (Hex)							
<b>Wire material</b>	Copper		Constantan harness		Constantan harness		Constantan harness		Copper		Copper				
<b>Lead gauge</b>	24 AWG		36 AWG		36 AWG		36 AWG		28/32 AWG		28/32 AWG				
<b>Signal amplitude</b>	Magnet	300 V pk	3 mV (300K) to 50 mV (4.2K)	0.1 V (77K) to 0.5 V (300K), actual excitation Current = 2.5 mA	0-5 V for resistance measurement the variation is 0-0.5 Ω or 10 μV – 1 mV (CFLA-6-350)	~ 2.0 mV/V	~ 2.0 mV/V	~ 2.0 mV/V	~ 1.00 mV/kG (at 298 K)	~ 1.00 mV/kG (at 298 K)	~ 1.00 mV/kG (at 298 K)				
	Dump R	250/500 Vpk													
	ZFCT	50 mV													
	PSU	6V													
<b>Sampling rate</b>	> 2 kHz		100 Hz		100 Hz		100 Hz		100 Hz		100 Hz				
<b>Excitation current/Voltage</b>	n/a		0.20-20 μA		1-5 mA		0-10 V (2.5 V)		0-10V (2.5 V)		100 mA				
<b>No. of channels</b>	24		71		61		38		26		12				
<b>Multiplexed</b>	YES / NO		Y		Y		Y		Y		Y				
<b>Control</b>	Primary-Hard wired to Quench detection/Secondary - PLC		PLC		PLC		PLC		PLC		PLC				
<b>Fast DAQ</b>	FPGA		FPGA		FPGA		FPGA		FPGA		FPGA				

**(B) SOLENOID magnet System**

Measurement	Voltage		Temperature (4 K)		Temperature (77K)		Load cell		Hall sensor						
<b>Sensor/Wiring Type</b>	8mil Kapton insulated-multi-strand copper wire (pair)		Cernox™ – 4 wire (4.2 – 325K)		Calibrated PT100 – 4 wire		LOAD CELL, 4 wire, 300 K (Force)		Cryogenics hall generator (axial), HGCA-3020, 4 wire						
<b># sensors/wiring</b>	Magnet	21	Magnet	26	Thermal shield	18	8 (LCM307)	0-10 kN (axial)	Vacuum Vessel	3	~ 1.00 mV/kG (at 298 K)				
	Zero-Flux Current Transducer, Power supply Bus	4					8 (KMR300kN)	0-165 kN (radial)							
<b>Wire material</b>	Constantan/Manganin/Copper		Constantan harness		Constantan harness		Copper		Copper						
<b>Signal amplitude</b>	Magnet	718 V pk	3 mV (300K) to 50 mV (4.2K)	0.1 V (77K) to 0.5 V (300K), actual excitation Current = 2.5 mA	~ 2.0 mV/V	~ 2.0 mV/V	~ 2.0 mV/V	~ 2.0 mV/V	~ 1.00 mV/kG (at 298 K)	~ 1.00 mV/kG (at 298 K)	~ 1.00 mV/kG (at 298 K)				
	Dump R	250/500 Vpk													
	ZFCT	50 mV													
	PSU	6V													
<b>Sampling rate</b>	> 2 kHz		100 Hz		100 Hz		100 Hz		100 Hz						
<b>Excitation current/Voltage</b>	n/a		0.20-20 μA		1-5 mA		0-10V (2.5 V)		100 mA						
<b>Control</b>	Primary-Hard wired to Quench detection/Secondary - PLC		PLC		PLC		PLC		PLC						
<b>Fast DAQ</b>	FPGA		FPGA		FPGA		FPGA		FPGA						

force action on valves, heaters, power supplies, etc. The PLC also serves this data for an EPICS input output controller (IOC) to allow for archiving and site wide system control (e.g. the cryo compressor in the end station refrigerator can use one of our liquid levels to help determine cryogenic heat load).

- In parallel another cRIO (fast DAQ) uses its 24-bit ADCs to monitor the VTs. This cRIO directly sends 10 kHz data to EPICS IOC for off-line consumption. In parallel, it also sends the voltage tap data to the

PLC at a rate of 5 Hz for the redundant (secondary) protection system.

- Analog data collection from other devices not listed above are:

- (i) Pressure transducers.
- (ii) Electric valves (EVs): each EV has an linear voltage displacement transducer which is used to set to determine valve position. EVs will retain their last position in the event of a power failure.

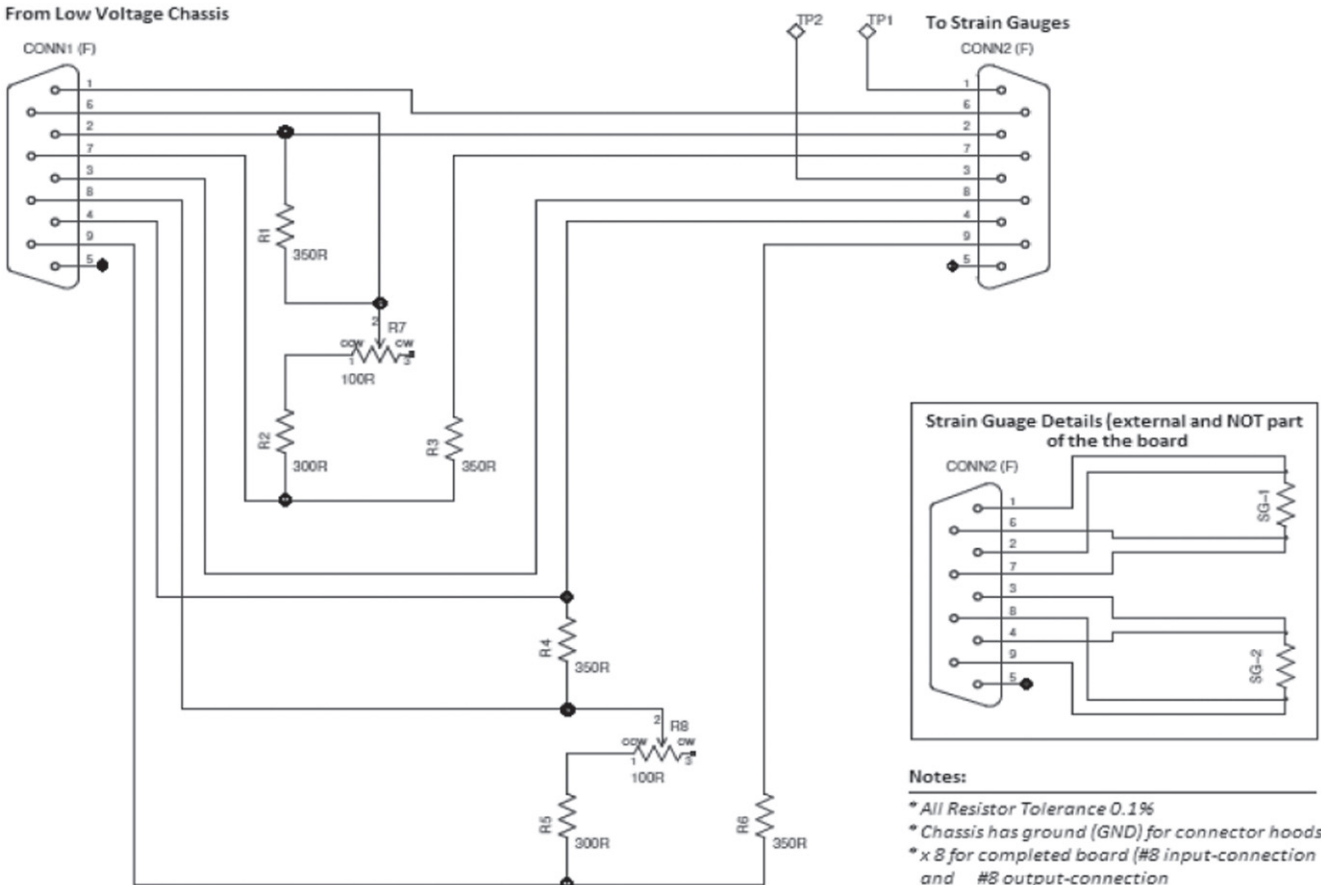


**Figure 15.** Schematic layout of the strain gauge bridge circuit module.

- (iii) Pneumatic valves (PVs): PVs are either fully open or fully closed. In the event of a power failure they will either close or open depending on their location within the cryogenic circuit.
- (iv) Pressure relief valves (RVs): each RV has a PT100 temperature sensor mounted on it so that if the valve freezes in the open position during a release of cryogens, the operator will be alerted and can take appropriate action—which usually involves applying a heat gun to the valve to unfreeze it.
- (v) Vapor cooled lead (VCL) heaters: each VCL has three set of heaters as part of the ice-management system (i.e. to prevent the build-up of large ice balls during operation). Two sets are controlled by a local set of controls while the third set is controlled by the PLC.
- (vi) VCL lead flow indicators: the cold helium gas which exhausts from the VCLs is warmed up to room temperature by flowing through a vaporizer before being routed through a set of calibrated helium gas flow indicators, figure 16(a).
- (vii) Vacuum pump control (gauges and gate valve): the pumps are controlled by a set of local controllers which can be accessed remotely by

- the PLC control system via ethernet. Similarly, the vacuum gauges are monitored remotely by the PLC. Should the vacuum level of the magnet vacuum space rise to an acceptable limit (excessive outgassing or an atmospheric leak for example), the gate valve would close to protect the turbo-molecular pump.
- (viii) Bus bar water flow switches: the pair of leads that connect the MPS to the magnet are cooled using low-conductivity water. The GO and RETURN leads each have their own water flow switch which will interface to an interlock to run the magnet down to zero current should the water flow fall below allowable limits. Each water-cooled lead also has a PT100 temperature sensor mounted on the lead terminal at the power supply end to act as a backup should the temperature of the leads exceed allowable limits which would once again initiate a controlled ramp down of the magnet.
- (ix) MPS water flow and temperature monitors: each MPS has its own set of internal sensors to monitor water flow, temperatures and voltages which operate an internal set of interlocks for additional protection.

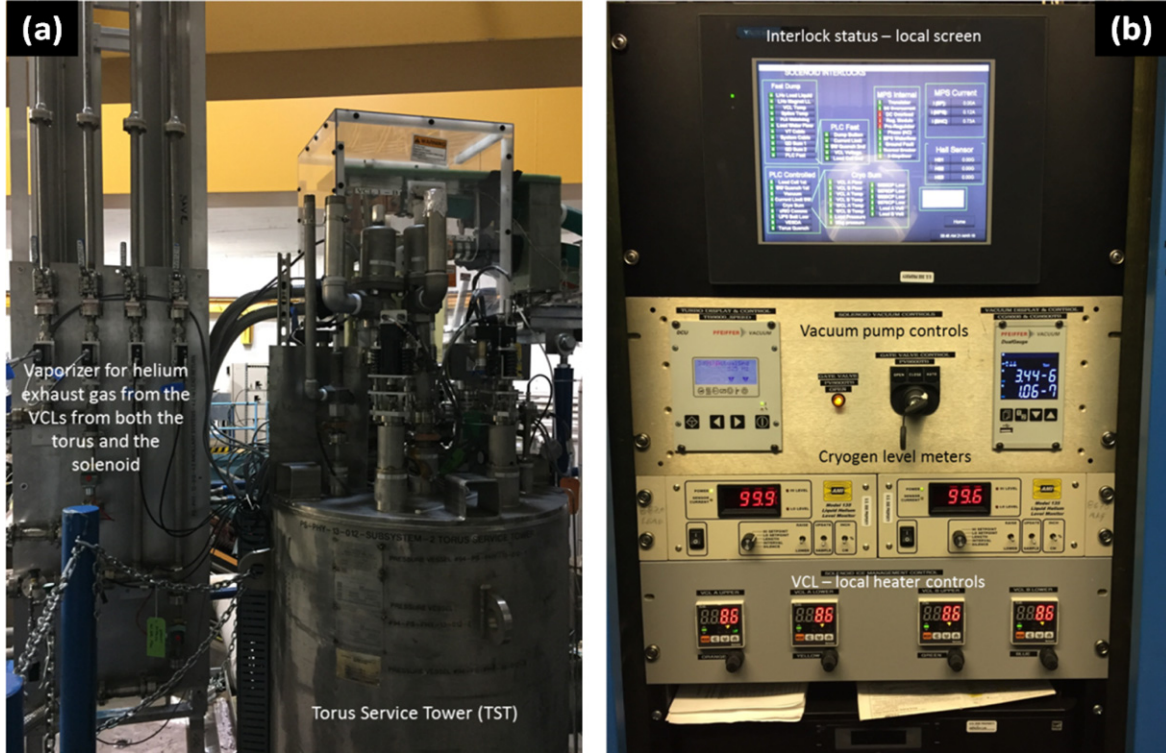


**Figure 16.** (a) Vaporizers for helium exhaust gas from VCLs, (b) solenoid vacuum pump controls, cryogen level meters, and VCL–local heater controls.

#### 4. Quench protection and control

##### 4.1. Magnet QPS

The magnet QPS (for both the magnets) is essentially an external system. On detection of a quench (via VTs which pick-up the growth of resistive voltages), a mechanically operated dump switch is opened to isolate the MPS from the magnet coils. The majority of the stored energy within the magnet is extracted and dissipated in an external dump resistor which is permanently connected across the terminals of the magnet. The remainder of the energy is dissipated within the magnet coils and cryogenic system itself. All joints (splices) between the individual superconducting magnet coils, between coils and current-leads and long runs of superconducting bus bar have additional copper stabilizer to manage temperature rises during a quench event. In fact, one of the key requirements for detection of a quench event and protection during a quench is the calculation of the amount of additional copper stabilizer to use. Too much copper, and the resistive voltage developed during a quench would be too low and thus difficult to detect. Conversely, too little copper would mean excessive temperature rise during a quench and a possible burn-out-of the conductor.

The designs of the quench protection and voltage tap sub-systems were driven by the anticipated levels of voltages developed during a magnet quench [8, 28]. Current limiting resistors are added in series to the VT wires in order to limit any potential current flow to less than 5 mA, which is the Class-I limit imposed by JLab's Environmental, Safety and

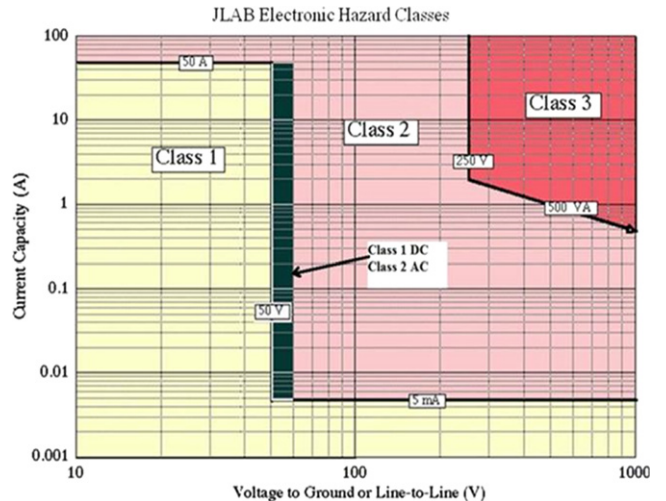


**Figure 17.** JLab electronic hazard class.

Health standards and is extracted from the National Fire Protection Association (NFPA) 70 NEC 2017 E—Standards for Electrical Safety in the Workplace [29]. Figure 17 summarizes the three classes for electronic equipment hazards.

As both the torus and solenoid magnets (and therefore VTs) could experience voltages in excess of 500 V, their complete voltage tap systems have been determined to fall into the equipment classes defined in table 8 by allowing for the following constructional details:

- The use of voltage tap cables possessing the appropriate insulation voltage rating;

**Table 8.** Equipment class for the Hall B to VT systems (for worst case quench scenario voltages).

Magnet	Maximum voltage (V)	Maximum current (mA)	Available energy during event (J)	Equipment class
Torus	580	5	9.67	Class 1
Solenoid	718	7.25	27.1	Class 2

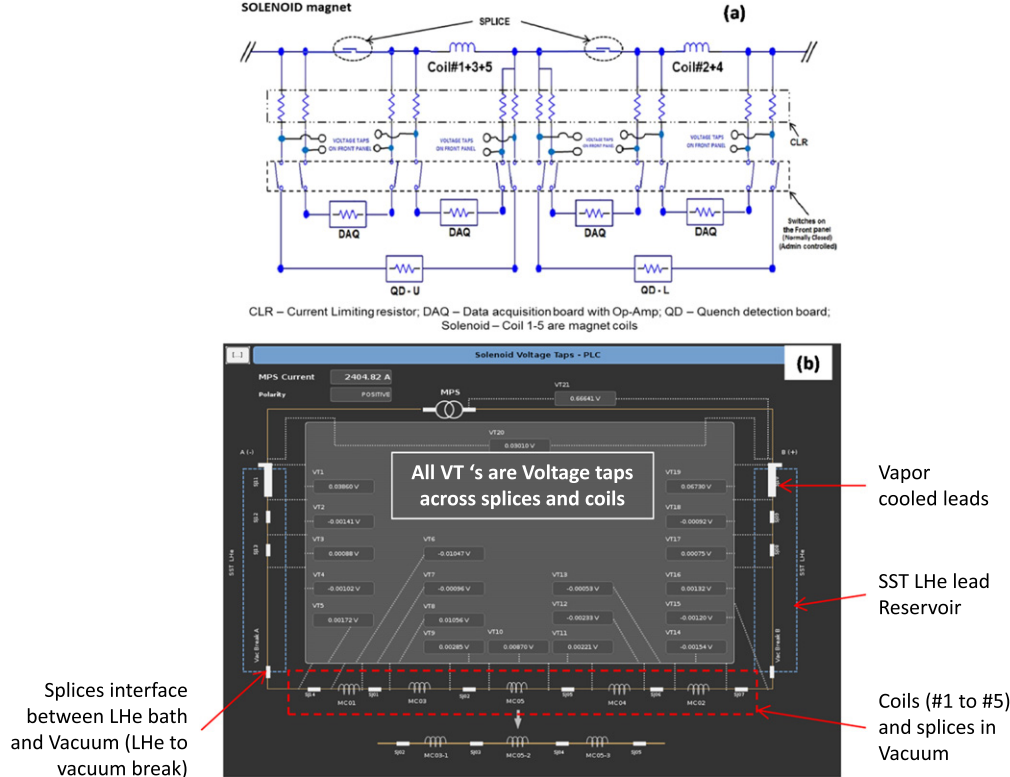


**Figure 18.** (a) Schematic arrangement of a typical section of the solenoid magnet for impedance-matching simulations: current limiting resistor (CLR), Op-Amp, QD board; (b) EPICS screen showing the voltage tap readouts for the solenoid (magnet shown in steady state operation).

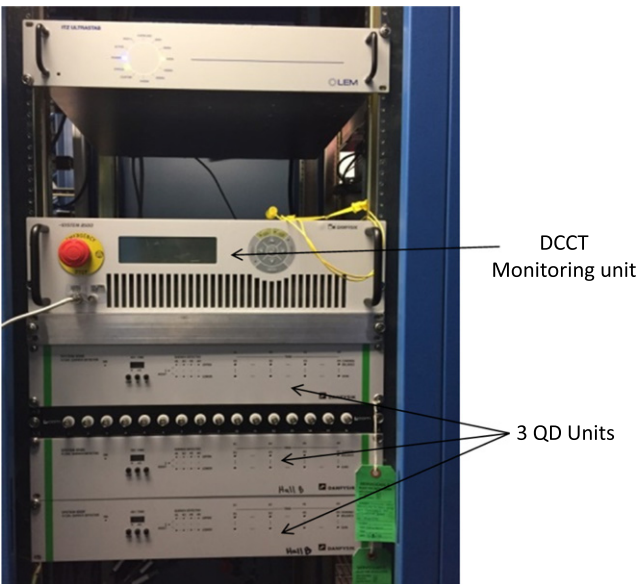


**Figure 19.** LEM Ultrastab direct current current transformer monitoring unit, remote control crate for magnet power supply, three quench detector units (each capable of monitoring four channels).

- (b) The use of current limiting resistors to limit current flow to no higher than 5 mA;
- (c) The use of administrative locks and tags on the feedthrough connectors;
- (d) Bolted panels on the voltage tap 19 inch rack systems.

The solenoid and torus utilize a dual quench protection scheme, where a primary analog (hardwired) circuit works in conjunction with a secondary digital PLC based circuit [30, 31]. Parallel path VTs from multiple locations throughout the magnet (magnet coils, splices, bus-bars, leads, etc) feed the primary and secondary quench protection sub-systems as represented in figure 18.

Figure 18(a) illustrates a simplified view of the five coils of the solenoid together with two splices. VTs (in pairs for redundancy) are shown on either side of each splice and coil set. These VTs (as pointed out earlier) incorporate an in-line current limiting resistor. All the VTs from the magnet coils and splices are terminated on a voltage tap break-out panel (also seen in figure 23). From that point, the VTs branch out into two paths. The first path feeds directly into the Danfysik QD modules (labeled QD-U and QD-L), see figure 19, and

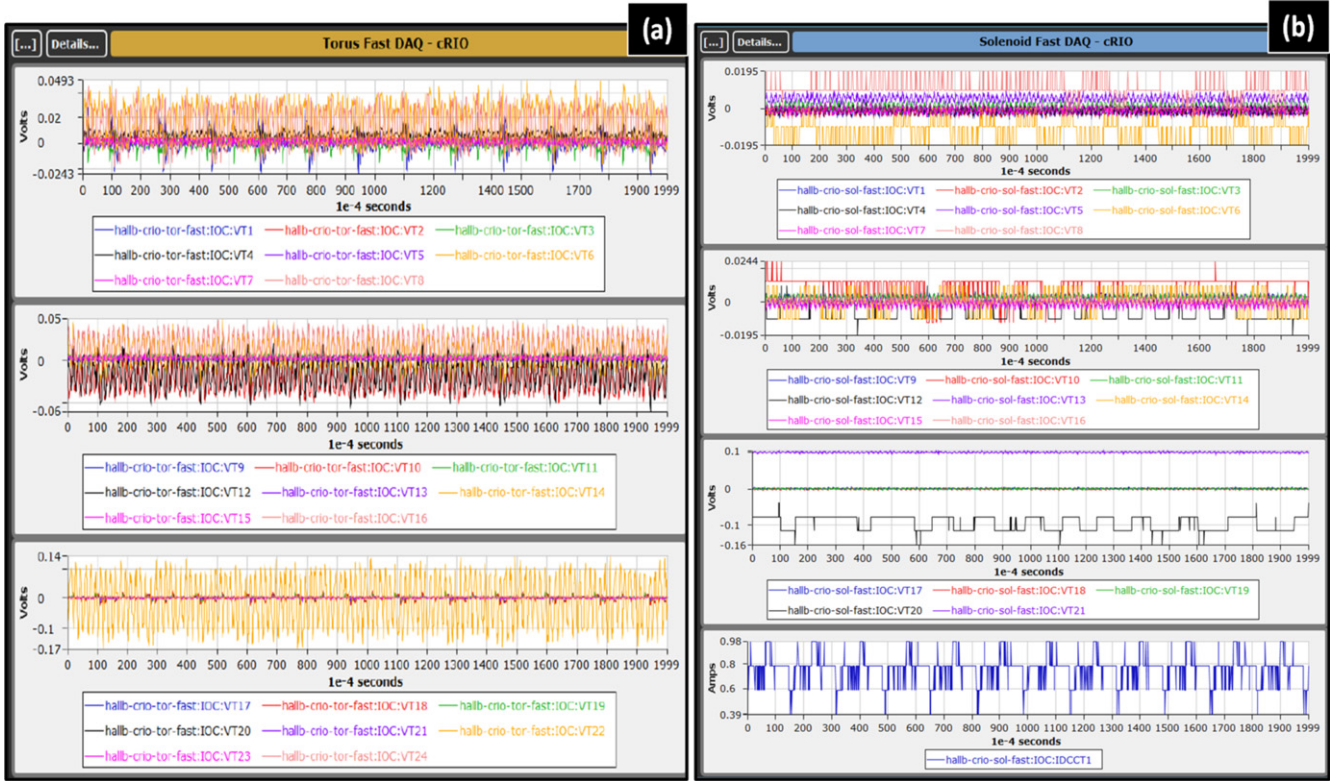


**Figure 20.** Screenshots of fast DAQ voltage tap data plots—examples shown here were captured during pre-commissioning while setting the voltage thresholds for the hardwired quench detectors—(a) torus and (b) solenoid magnet.

forms the primary (or hardwired) portion of the QPS. There are no intermediate electronics (for example network switches or isolation amplifiers) or software involved in its decision-making process. Furthermore, all system cables (including all voltage tap cables) are interlocked so that if even one cable is not connected, the protection system will not allow the magnet to be energized.

Each QD module consists of four differential input channels, i.e. an upper and lower channel. The voltage signals are fed into the lower and upper channels and then subtracted from each other. The resultant voltage is compared with the pre-set voltage threshold (i.e. set by the operator). If the resultant voltage is higher than this threshold and remains above this threshold for a pre-set time period, then the QD will trip (or fast dump) the magnet—i.e. the dump switch will open and the magnet will run down through the external dump resistor. Figure 18(b) illustrates the QD (VT) control screen which displays the whole solenoid magnet (with all five coils) together with all the VTs employed on the magnet.

Multiple simulations were carried out using LT Spice in order to mitigate the impedance-mismatch across every channel while considering the impedances from the DAQ system and QD units. The impedances from the DAQ and the QD will always be present during normal operation in order to comply with the aforementioned NFPA 70E requirements. The QD and DAQ systems in parallel result in a complex voltage divider network which requires modifications in order to balance the circuits. To modify the QD boards to comply with Class-I requirements, it was necessary to overcome the

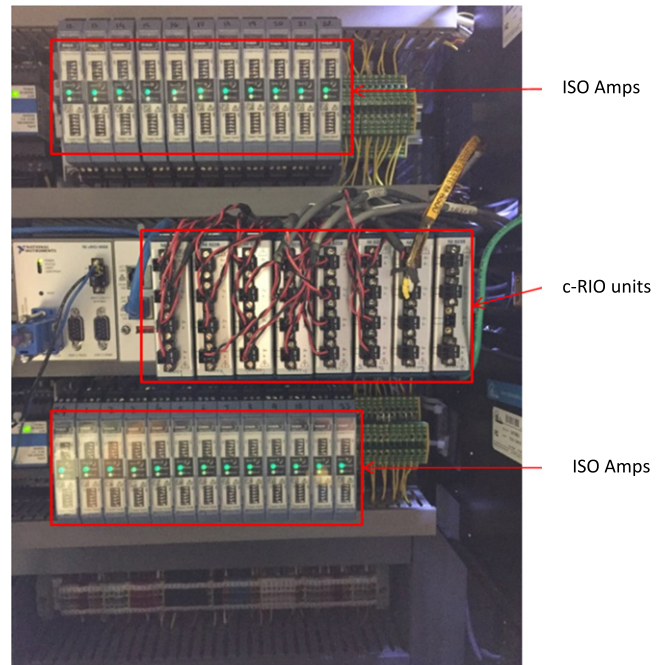


**Figure 21.** Fast DAQ (NI-cRIO) reading voltage tap data at the center of the picture. Isolation amplifiers are shown above and below the c\_RIO unit.

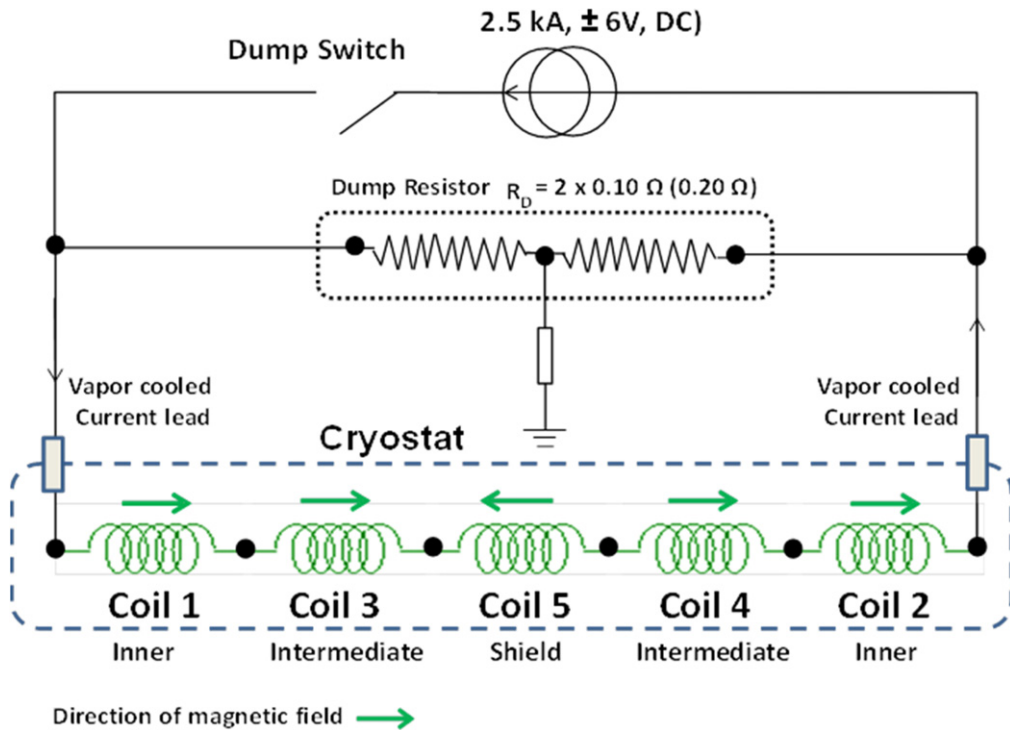
balancing issue across all the VTs in the QD units that share a common node with DAQs in parallel [30]. Fine tuning of the threshold voltages in the QDs was carried out during the pre-commissioning stages, after evaluating the noise across each

**Table 9.** Torus and solenoid magnet hardware and software interlock thresholds.

Torus magnet system			
	Acceptable operating range	Actual trip limit	Expected threshold
Hardwire interlocks (fast dump)			
Liquid helium level (superconducting probe)	21%–110%	<20%	<20%
Liquid helium level (differential pressure)	21%–110%	<20%	
VCL temperature	4.5–15 K	>15 K	>10 K
Danfysik QDs	>200 mV, 100 mV (VCL), >2250 mV		Varies across sections identified
PLC Interlock-I (fast dump)			
Current limit (hard coded)	Not to exceed $\pm 3880$ A	3850 A	$\pm 3880$ A
Software quench, second threshold	Coil voltages are compared >350 mV, VCL >125 mV		Coil voltages are compared >350 mV, VCL >125 mV
PLC interlock-II (controlled ramp down)			
CCM load cell	Top 600 lbs, bottom 1300 lbs	Top 600 lbs, bottom 1300 lbs	Top 600 lbs, bottom 1300 lbs
Vertical support	–9500 lb		–9500 lb
Coil comparators first threshold	Coil voltages are compared >250 mV		Coil voltages are compared >250 mV
Vacuum	$>5 \times 10^{-5}$ Torr		$>5 \times 10^{-5}$ Torr
Pressure helium tank	PT8120 < 2.3 atm		PT8120 < 2.3 atm
Supercritical helium pressure	2.4–3.0 atm	<2.3 atm	
Pressure nitrogen tank	<2.0 atm		<2.0 atm
Liquid level (LL) helium tank	<90%		<90%
LL nitrogen tank	<90%		<90%
VCL flow	$\pm 15$ standard liters per minute (SLPM) of set point (SP)		$\pm 15$ SLPM of SP
VCL temperature	>10 K		>10 K
VCL voltage	80 mV		80 mV
Solenoid magnet system			
Hardwire interlocks (fast dump)			
Liquid helium level (superconducting probe)	21%–110%	<20%	<20%
Liquid helium level (differential pressure)	21%–110%	<20%	
VCL temperature	4.5–20 K	>20 K	<15 K
Danfysik QDs	>200 mV, 100 mV (VCL), >1500 mV		Varies across sections identified
PLC interlock-I (fast dump)			
Current limit (hard coded)	Not to exceed $\pm 2500$ A	2500 A	$\pm 2500$ A
Software quench, second threshold	Coil voltages are compared >350 mV, VCL > 125 mV		Coil voltages are compared >350 mV, VCL > 125 mV
PLC interlock-II (controlled ramp down)			
Axial support	0–8000 lbs		
Radial support	0–18 000 lbs		
Coil comparators first threshold	Coil voltages are compared > 250 mV		Coil voltages are compared >250 mV
Vacuum	$>5 \times 10^{-5}$ Torr		$>5 \times 10^{-5}$ Torr
Pressure helium tank	PT8120 < 2.3 atm		PT8120 < 2.3 atm
Supercritical helium pressure	2.4–3.0 atm	<2.3 atm	
LL helium tank	<90%		<90%

**Table 9.** (Continued.)

Torus magnet system			
	Acceptable operating range	Actual trip limit	Expected threshold
VCL flow	$\pm 15$ SLPM of SP	$\pm 15$ SLPM of SP	
VCL temp	4.5–15 K	>17 K	
VCL voltage	80 mV	80 mV	

**Figure 22.** General electrical connection of the solenoid magnet, power supply and dump resistor.

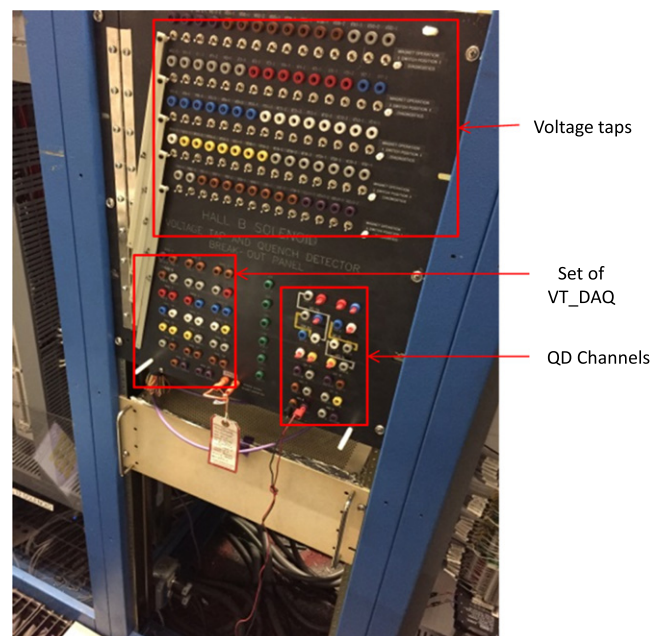
channel in the system. The values are based on the measured data from the fast DAQ system as shown in figure 20.

The secondary QD system routes voltage tap data from the magnet via Knick isolation amplifiers (iso-amps) to a second dedicated NI-cRIO having eight four-channel N9239 24-bit analog input modules, figure 21. The voltage tap data are then manipulated by the PLC to produce summed and subtracted voltages which are then routed to the various interlocks.

Two sets of thresholds are employed here:

- (a) one set to initiate a controlled ramp down; and
- (b) a second set which is deployed as a backup for the hardwired QD and also acts directly on the fast dump contactor.

The same cRIO also feeds VT waveform data to EPICS at 10 kHz for online review via parallel ethernet communications. The primary and secondary voltage thresholds for the torus and solenoid are given in table 9, which also provides the full list of interlocks that are managed by the control system.

**Figure 23.** Voltage tap break-out panel for the solenoid.

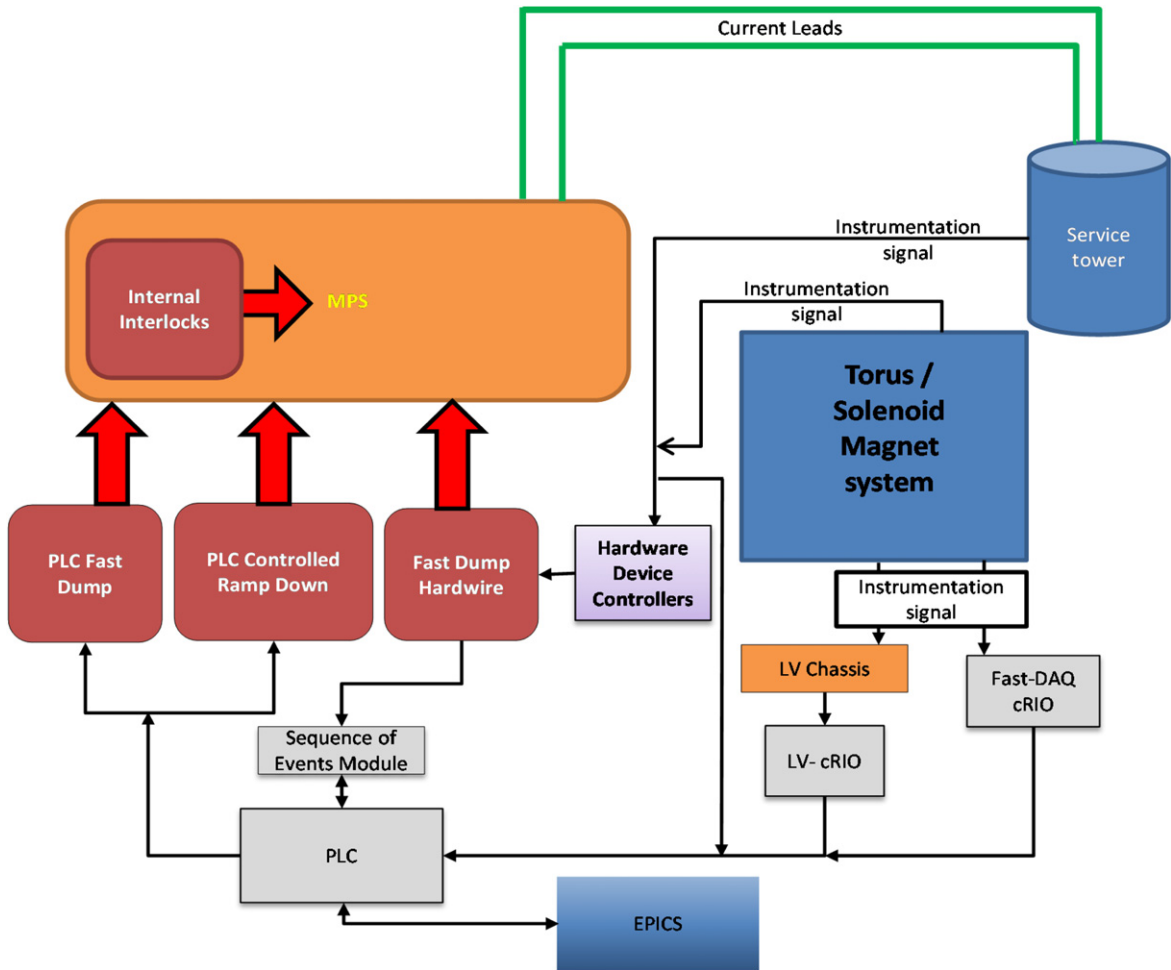


**Figure 24.** Global architecture of the torus and solenoid magnet interlock system.

A quench-induced voltage which exceeds pre-set voltage thresholds for a certain time period will trigger the primary system closely followed by the secondary system. The dump switch will then be opened to isolate the power supply from the magnet and the majority of the stored energy will be dissipated within an externally connected dump resistor—which, by the way, is permanently connected across the magnet as additional protection. This of course means that the dump resistor will always be carrying some current during magnet operation. Figure 22 illustrates the general electrical connections for the solenoid magnet and also shows the center-point tap on the dump resistor which is connected to ground via a ground fault detection circuit resistor. There are no additional grounding points on the superconducting coils and the insulation system has been designed to withstand several kilovolts. The torus magnet circuit is similar and its coil insulation system is also similarly rated.

One of the major requirements for the solenoid and torus magnets with regards to the QD system was to have ready access to all the VTs on the magnets to enable easier magnet diagnostic measurements during pre-commissioning activities. This was achieved by introducing a manually switched voltage diagnostics panel (figure 23) between the magnet and the electronics. Landing the VTs on the voltage diagnostics

panel required that we reduced the level of hazard associated with medium to high voltages that could develop across magnet coils during a quench event from Class-II to Class-I based on NFPA 70E guidelines. This was accomplished by implementing administrative controls for this voltage tap panel.

The quench protection instrumentation (primarily the VTs and temperature sensors) provides valuable data during a quench event via data capture of the voltage and temperature waveforms. Information such as which coil quenched and hot spot temperatures are readily available by examination of the data after the event. The magnets are continuously monitored during ramp up, steady state operation and also ramp down—i.e. the QPS is always active—so inductive voltages across coils during ramp up and down operations are also captured and have been used during the commissioning process to ensure balance of voltages between the various coils and thus QD channels.

#### 4.2. Magnet control system (MCS)

The combined functions of the QPS and MCS ensure that each magnet is protected under any fault conditions (voltage, liquid level, current lead temperature, vacuum, quench). A fault on any device monitored by the QPS and MCS

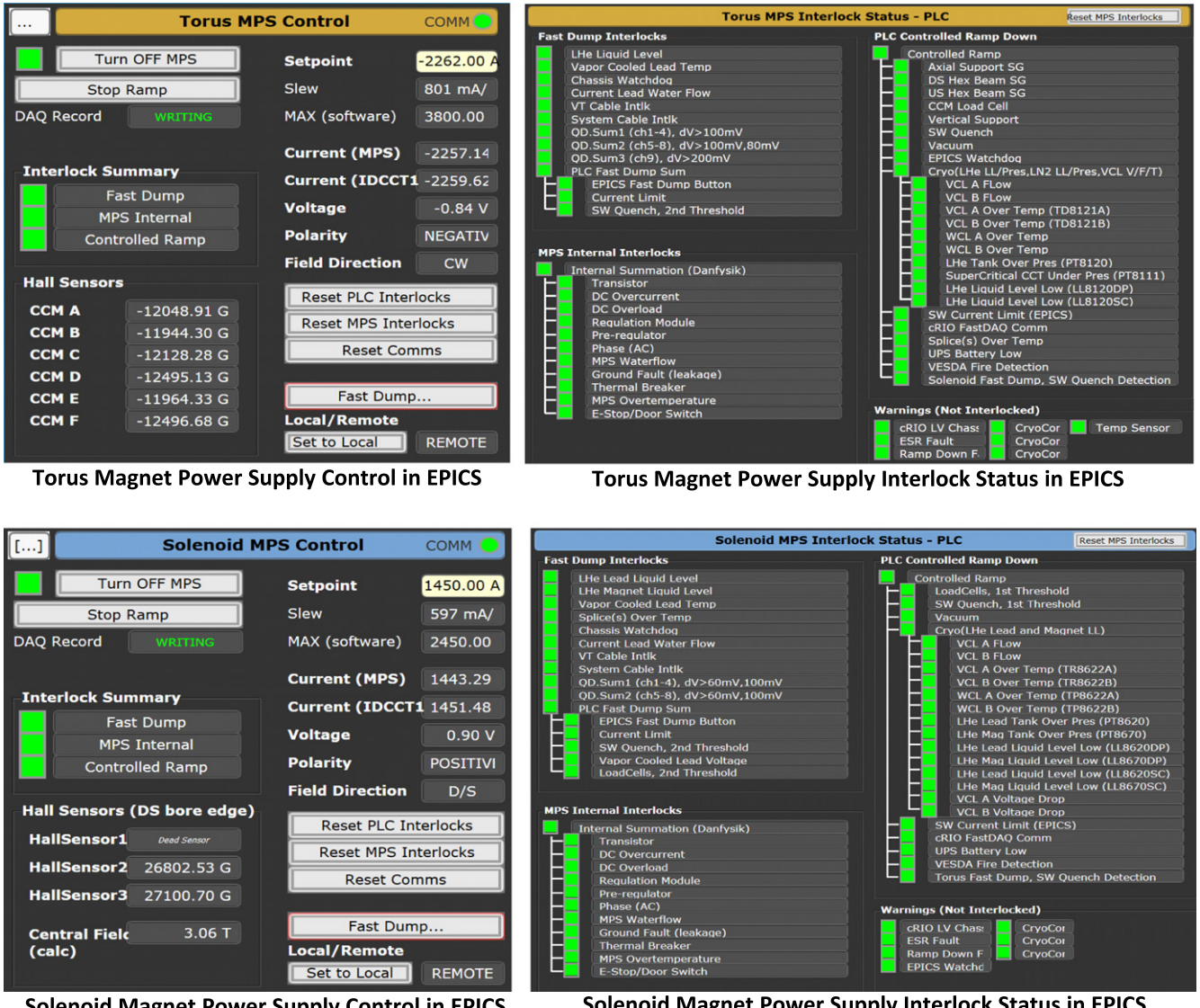


Figure 25. Magnet power supply control and interlock status screens (torus and solenoid).

automatically opens the dump contactor in the power supply, discharging the magnet through the dump resistor. The selection of devices to include in the MCS was driven largely by the FMEA process.

The torus and solenoid magnet interlock architecture is shown in figure 24. Any fast dump event from hardwired protection is registered in the sequence of events monitor and transferred to the PLC and EPICS for real-time display and archiving. An alarm manager is also used within the EPICS system to send out warnings and alarms via text and email.

The magnet power and cryogenic control systems are implemented in an Allen Bradley Control-Logix 1756-L72 Controller with Rockwell Automation software to program the PLC and to enable viewing of the status in real-time. Functions such as magnet interlocks and cryogenic interlocks act locally and independently of remote interfaces. Sensor instrumentation is routed into the PLC via NI-cRIO (FPGA/RT application) using the MSELV chassis. Configuration, monitoring, operator interface, alarm handler and archiving

system for each magnet system is provided by the EPICS. MPS control (via EPICS) and the PLC interlock status screens for both the torus and solenoid are shown in figure 25.

#### 4.3. DC power and dump switch

The power supply used for the torus and the solenoid magnets is a Danfysik 8500 rated at 4000 A, 6 V. This power supply is integrated with a dump resistor of 124 mΩ for the torus and 200 mΩ for the solenoid [32]. The primary QPS is hardwired, incorporated within the Danfysik power supply with a trigger threshold voltage that is adjustable. The redundant secondary QPS operates via the fast DAQ sub-system to the PLC that also can be used to trigger the dump switch or to initiate controlled ramp down.

The mechanical dump switch, as supplied by Danfysik and located within the main power supply cabinet, consists of three spring-loaded arms. Tests of the power supply into a dummy resistive load indicated that the total time delay from a voltage exceeding a set threshold to the dump switch being

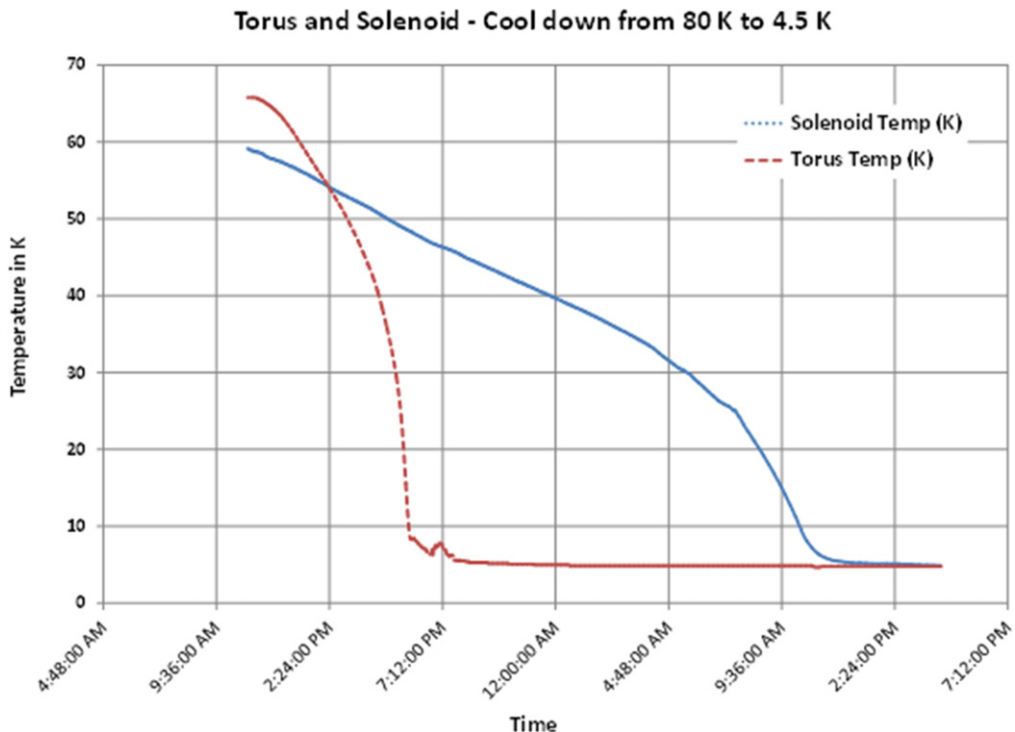


**Figure 26.** Torus and solenoid—cool down from about 80 K to 4.5 K.

fully opened was of the order of  $>700$  ms, which was deemed to be too long from a coil quench hot spot temperature rise point of view:

$$T_{\text{total}} = T_{\text{qi}} + T_{\text{dsw}} > 700 \text{ ms, where}$$

$T_{\text{qi}}$  = time between when the quench voltage threshold is exceeded to when the ‘quench interlock’ contact opening is relayed to the power supply,

$T_{\text{dsw}}$  = time between a quench interlock being relayed to when the dump switch is fully opened.

The circuitry controlling the relay to the dump switch was modified by JLab to reduce this time delay under instruction from the power supply vendor. Final tests of the power supply and subsequent measurements during commissioning of the magnets confirmed that the new shortened time delay was about 120 ms which provided a healthy safety margin.

#### 4.4. AC mains and uninterruptable power supply (UPS)

The PLC, cRIO, and associated control hardware are all on a UPS backup power. Additionally the mains power is backed up with a backup generator. In the case of a mains power outage and generator failure, the PLC will use a battery low signal from the UPS to ensure a safe ramp down of the magnet current and initiate safe valve positions for the cryogenic and vacuum systems.

### 5. Discussion—commissioning results

As with any typical project, the key drivers were technical reliability, schedule and cost. These drivers encouraged the

team to adopt the FMEA methodology to assist with design and instrumentation choices. In practice, this methodology was also used during the installation and commissioning stages for both magnets to great advantage.

Establishing the minimum number of temperature sensors and ideal locations on the magnet coils allowed the team to monitor and control the cool down of these magnets in order to minimize temperature differentials across the coils and thereby minimize thermal stresses.

The decision, taken early on in the project cycle, to test the individual torus coils to only 80 K was demonstrated during commissioning to be a sound decision, from a balanced consideration of technical performance, cost and schedule. The 80 K cool down test and strategic placement of temperature sensors helped to establish safe cool down rates and temperature differentials across the coils. The results from finite element studies, the output from the FMEA process and the results from the 80 K cool down and electrical tests all served to reduce the key technical risks (cooling efficacy, temperature distribution, thermal stresses and insulation integrity). In fact, these cool down guidelines were subsequently applied to the solenoid also with great success.

From room temperature to about 80 K or so, cool down rates of  $1\text{--}3 \text{ K h}^{-1}$  were used coupled with temperature differentials across the cold mass of no higher than 30 K or so. The cool down time from 300 K to about 4 K for the torus was calculated to be about 14 d assuming a maximum temperature differential across the cold mass of 30 K and helium flow rate of  $7.0 \text{ g s}^{-1}$ . In reality, the cool down took longer and was carried out in several steps. During the cool down process (average CCM temperature = 209 K), it was noted (via observation of strain gauge readings on the

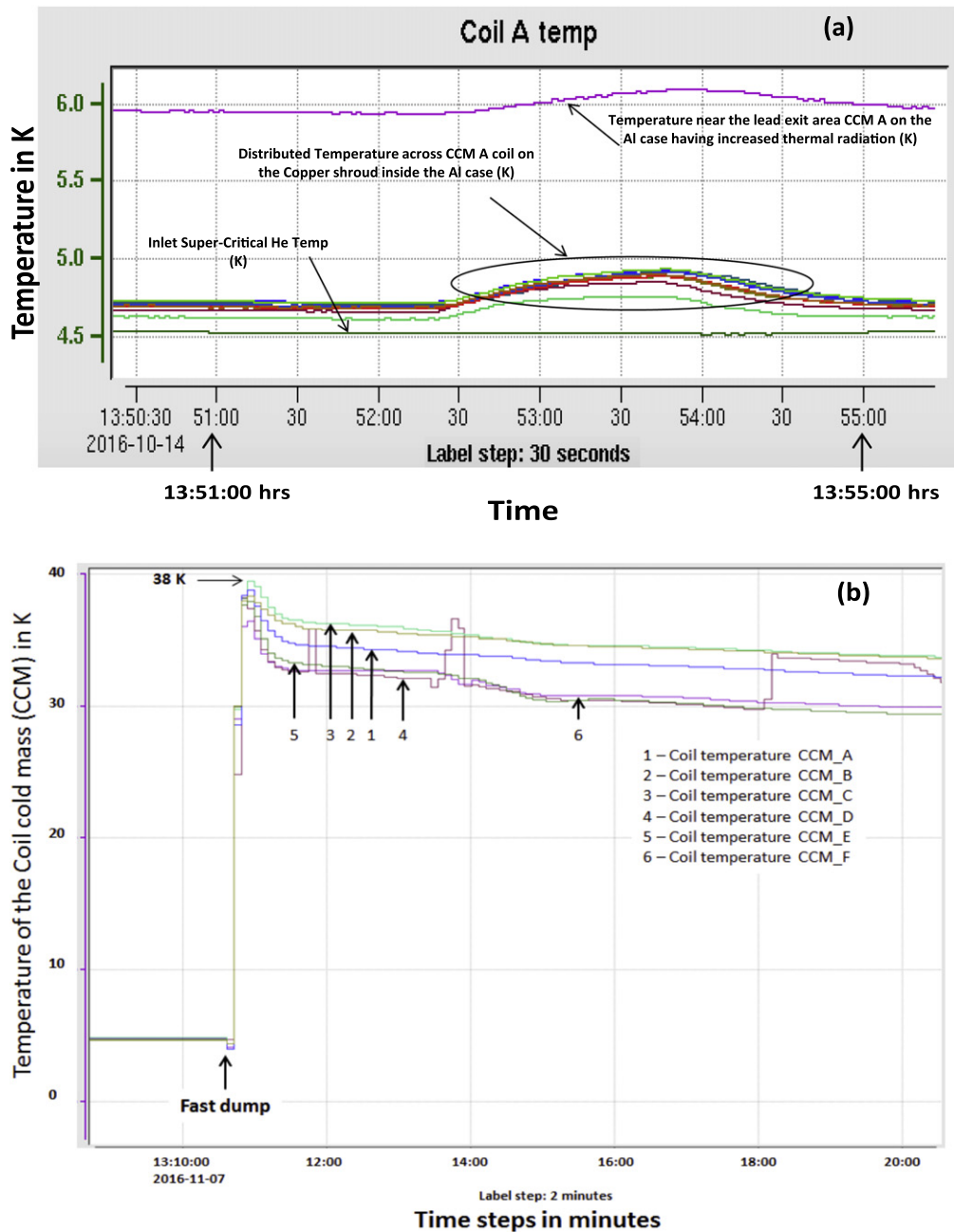


**Figure 27.** Torus: (a) temperature rise of CCM A during ramp to 300 A at  $2 \text{ A s}^{-1}$  due to eddy current heating. (b) CCM maximum temperature during a fast dump from 3000 A.

supports) that the four torus vertical supports were apparently bending. This necessitated a slow-down in the cooling process (to about 170 K) and finally a temporary halt while measurements and strain gauge calibrations were checked. It was discovered that although some of the strain gauges were not being adequately temperature compensated, the vertical supports were indeed experiencing some level of bending. A risk review was convened to plan the path forward and four options were considered, which included a ‘worst’ case option that required a warm-up to room temperature to repair the vertical supports by cutting into the vacuum jacket. A spare vertical support was tested at liquid nitrogen temperature and was demonstrated to have a

more than adequate strength safety factor under bending. It was thus determined that it was safe to continue with the torus cool down which was then resumed and the torus achieved its helium operating temperature of 4.5 K without any further issues.

Figure 26 indicates the cool down curves for both the torus and solenoid magnets from about 80 to 4.5 K. It can be seen that once the torus got to 80 K or so, it only took another 12 h or so to get down to 4.5 K which was achieved by increasing the flow of helium to the magnet. The solenoid cool down from 300 K to 4 K took a total of about 20 d—additional care had to be taken with Coil 5 as it lagged behind the rest of the main cold mass (i.e. Coils 1–4), being at the

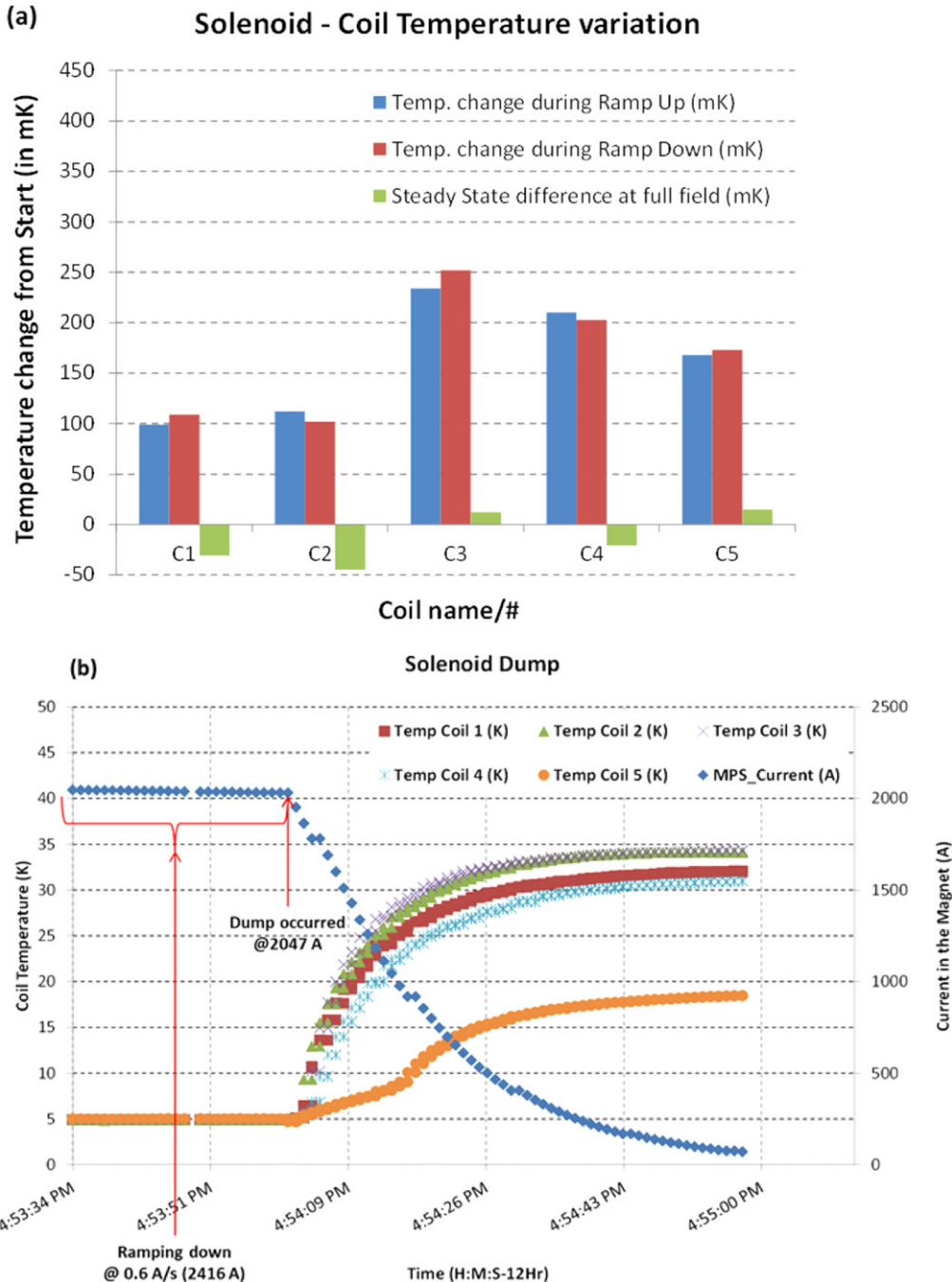


**Figure 28.** (a) Solenoid: rise in coil temperature during ramp up, ramp down and at steady state after upon reaching full operating current. (b) Solenoid: coil temperature rise during fast dump while ramping down the magnet.

end of the main cooling loop. The solenoid did not have any issues during the cool down process.

The torus magnet was commissioned successfully in November 2016 with zero quenches. There were however several fast dumps (most of which were planned as part of the commissioning process) at different currents during the ramp up to field. Several controlled ramp-downs were also initiated as interlocks were triggered either due to an initial overly sensitive setting of thresholds or by a cryogenic perturbation elsewhere in the system. These events allowed the team to fine-tune settings and thresholds to minimize the number of fast dumps and controlled ramp-downs.

For the torus magnet, eddy current heating during a ramp up to field was observed on the CCMs. Figure 27(a) indicates a temperature rise of about 0.3 K. The ramp rates were varied during commissioning in order to minimize these eddy current effects and to establish the safe operating envelope for the magnet. The maximum recorded temperature measured on the CCMs during a fast dump from 3000 A was about 40 K as shown in figure 27(b). The fast dump data proved to be in good agreement with the detailed predictive model [8].

The solenoid magnet was commissioned in September 2017 and underwent a similar commissioning process. Once again eddy current heating during ramp up to field was

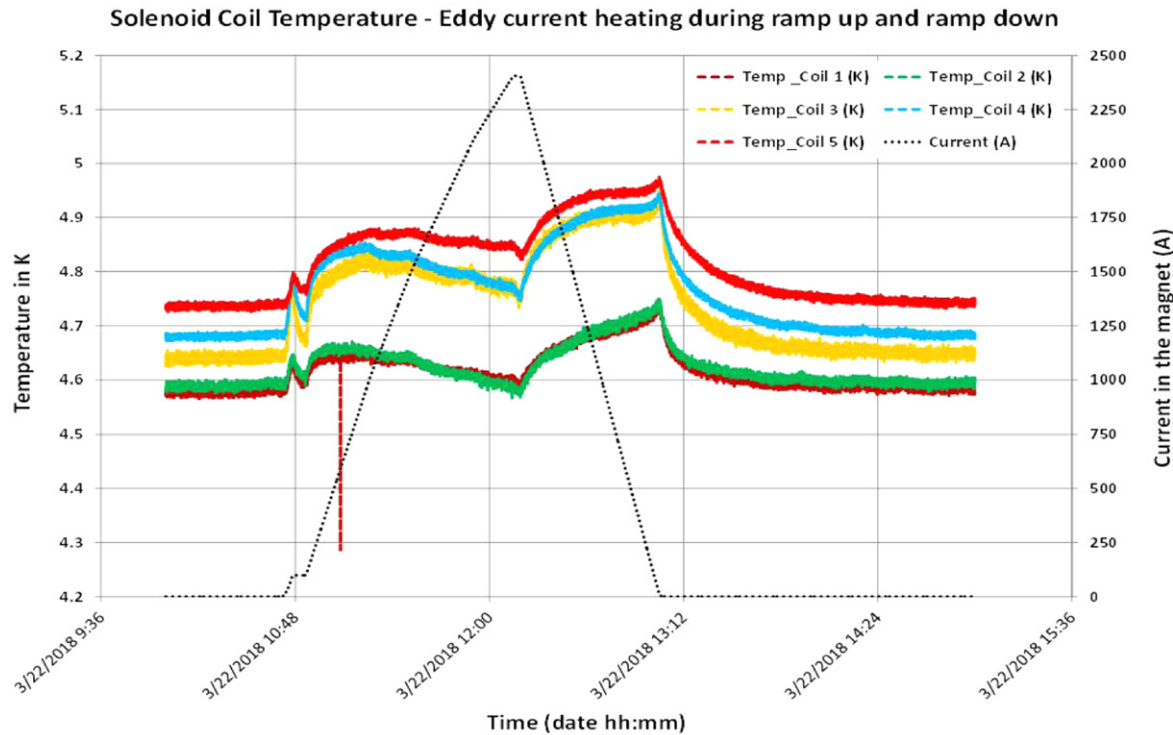


**Figure 29.** Rise in solenoid coil temperature during ramp up to full operating current of 2416 A, followed almost immediately by a controlled ramp down.

observed. The maximum temperature rises measured for all five coils is as shown in figure 28(a), during a ramp up to 1460 A, with a ramp rate of  $0.7 \text{ A s}^{-1}$  up to 900 A and  $0.6 \text{ A s}^{-1}$  up to 1460 A. The ramp rate was subsequently decreased to  $0.5 \text{ A s}^{-1}$  up to 2100 A and  $0.4 \text{ A s}^{-1}$  to full field to minimize rise in coil temperature. During a ramp down of the solenoid from full current (2416 A), a fast dump was triggered at about 2047 A (by a spurious voltage spike) and caused the temperature in Coils 1–4 to rise to about 35 K or so while Coil 5 increased in temperature to about 19 K, figure 28(b). Quench analyses predict that a quench from full field (2416 A, 5 T) would cause a temperature peak of about 50 K.

A graphical inspection of the solenoid coil temperature rises during a ramp to the full operating current of 2416 A and also during a controlled ramp down is shown in figure 29. The controlled ramp down is a straight ramp down to zero amps by the power supply (i.e. not through the dump resistor which is what happens during a fast dump). The temperature rises were modest (no higher than about 0.3 K) and well within the calculated 1.2–1.5 K temperature margin of the coils.

Load cell selection and calibration in a magnetic field prior to installation on the torus and solenoid was a major factor in obtaining reliable and reproducible readouts throughout the cool down and energization phases of commissioning. Figure 30 shows the change in the OOPS load cell readings for CCM A during a ramp up to the full operating current of 3770 A followed by a controlled ramp down to zero amps. As expected, there is only a minimal force experienced by the coil within its vacuum jacket during energization. This behavior is demonstrated by all six coils

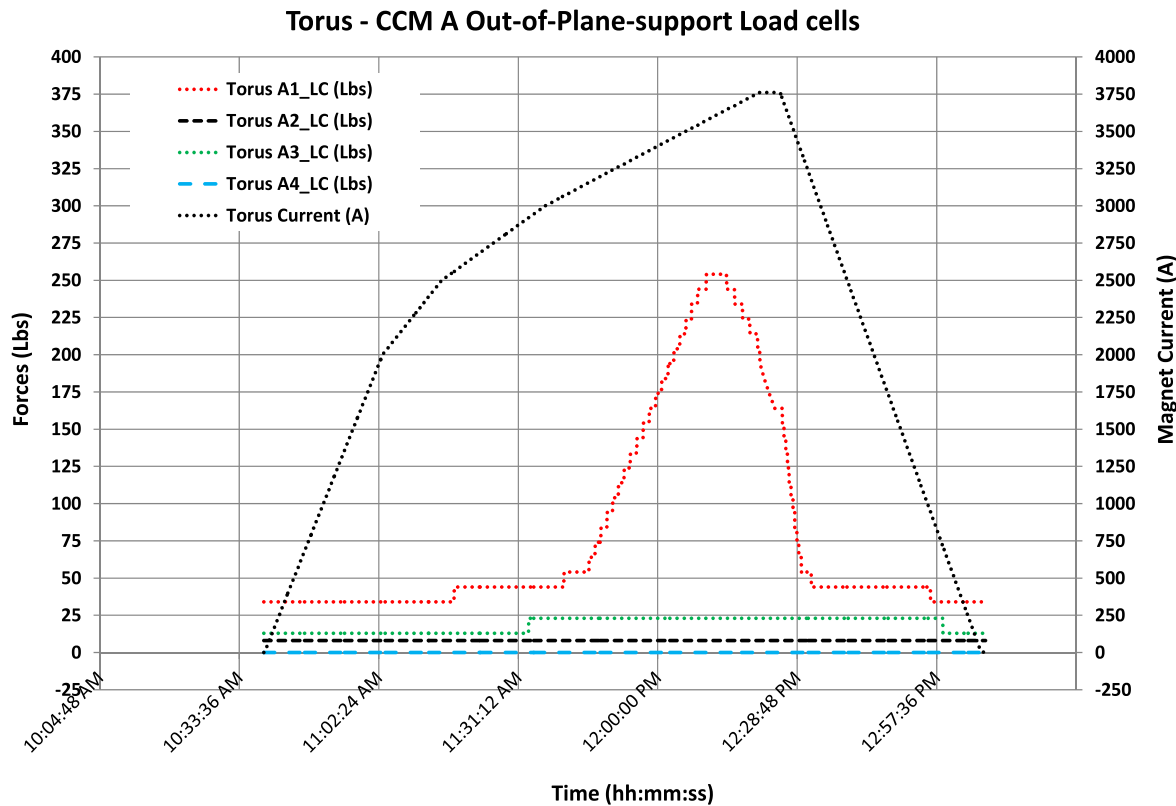
with only minor variations depending on the location of the coil due to gravity loading. This behavior was also noted to be extremely repeatable following many cycles of magnet energization and de-energization.

Figure 31 shows the change in the radial and axial load cells on the solenoid during a ramp up to the full operating current of 2416 A followed by a controlled ramp down to zero amps. It is encouraging to note that all the forces revert back to almost the original values after de-energization illustrating that none of the coil support structures has yielded and it has also been shown from subsequent runs that this process is very repeatable.

## 6. Summary

The complexities of both magnet systems, necessitated complete and thorough RAM during all stages of conceptual and final design, manufacture, installation, commissioning and operation. A detailed FMEA process provided critical guidance in the selection of suitable instrumentation hardware, appropriate quality assurance and quality control procedures during manufacture and installation and for the overall protection of the magnets and their sub-systems.

Both the torus and solenoid were installed and commissioned successfully in November 2016 and September 2017 respectively. Experimental physics runs are now underway with both magnets functioning within as-designed parameters at full field, in both polarities.



**Figure 30.** Torus: change in CCM A OOPS load cells during ramp up to the full operating current of 3770 A, followed by a controlled ramp down to zero amps.

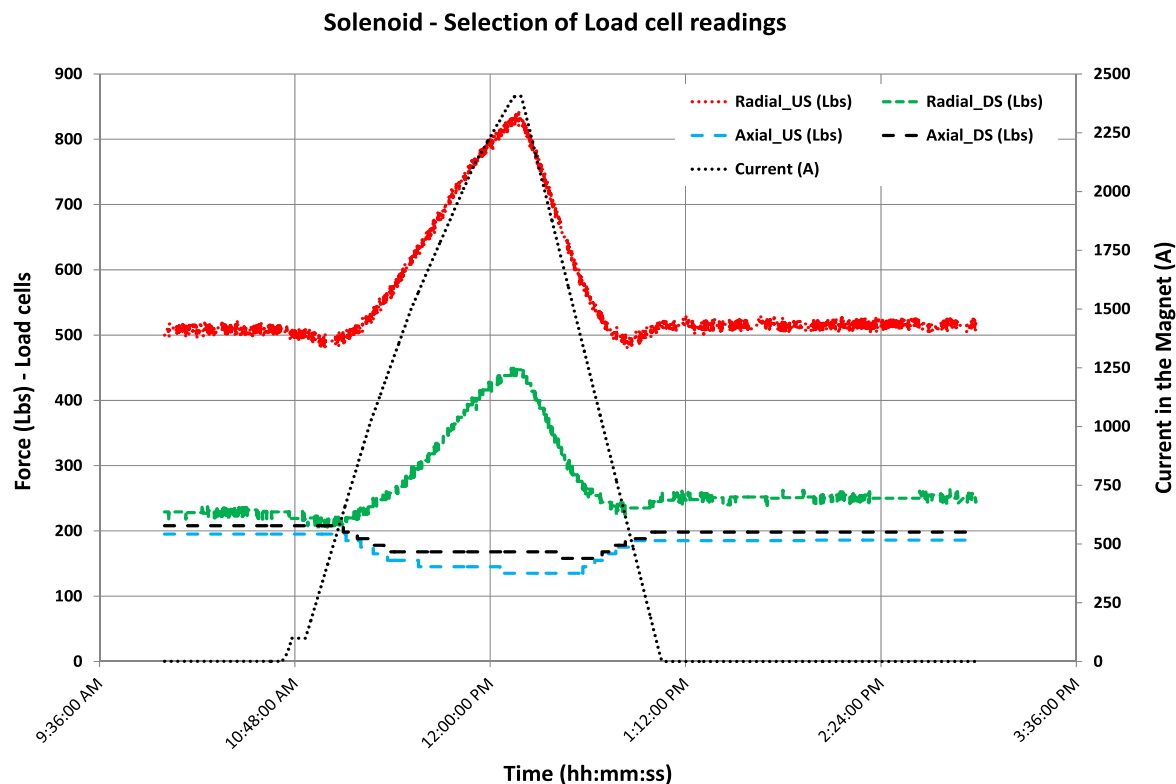


**Figure 31.** Solenoid: selected load cells readings during ramp up to full operating current of 2416 A, followed by a controlled ramp down.

## Acknowledgments

The authors would like to acknowledge the contributions and support from all Hall B staff, Detector Support Group people and technicians at JLab. The authors would like to thank C Rode (JLab-retired), V Rao-Ganni (MSU), J Creel (JLab), G Biallas (JLab-retired), C Luongo (presently at ITER), M Mestayer (JLab), R Flora (FNAL), S Prestemon (LBNL) for their valuable suggestions and critical discussion during the process of FMEA and system review. This material is based upon work supported by the US Department of Energy, Office of Science, Office of Nuclear Physics under contract DE-AC05-06OR23177. The US Government retains a non-exclusive, paid-up, irrevocable, world-wide license to publish or reproduce the published form of this manuscript, or allow others to do so, for United States Government purposes.

## ORCID iDs

Probir K Ghoshal  <https://orcid.org/0000-0002-4441-6388>

## References

- [1] Fair R J and Young G L 2015 Superconducting magnets for the 12 GeV upgrade at Jefferson Laboratory *IEEE Trans. Appl. Supercond.* **25** 4500205
- [2] Luongo C et al 2016 The CLAS12 torus detector magnet at Jefferson Lab *IEEE Trans. Appl. Supercond.* **26** 4500105
- [3] Krave S et al 2016 Overview of torus magnet coil production at Fermilab for the Jefferson Lab 12 GeV Hall B upgrade *IEEE Trans. Appl. Supercond.* **26** 4102705
- [4] Ghoshal P K et al 2015 FMEA on the superconducting torus for the Jefferson Lab 12 GeV accelerator upgrade *IEEE Trans. Appl. Supercond.* **25** 4901005
- [5] Ghoshal P K et al 2015 Electromagnetic and mechanical analysis of the coil structure for the CLAS12 torus for 12 GeV upgrade *IEEE Trans. Appl. Supercond.* **25** 4500705
- [6] Pastor O, Willard T, Ghoshal P, Kashy D, Wiseman M, Kashikhin V, Young G, Elouadrhiri L and Rode C 2015 Structural analysis of thermal shields during a quench of a torus magnet for the 12 GeV upgrade *IEEE Trans. Appl. Supercond.* **25** 4500404
- [7] Rajput-Ghoshal R, Ghoshal P K, Fair R J, Hogan J and Kashy D 2015 An investigation into the electromagnetic interactions between a superconducting torus and solenoid for the Jefferson Lab 12 GeV upgrade *IEEE Trans. Appl. Supercond.* **25** 4100605
- [8] Ghoshal P K, Biallas G, Fair R J, Kashy D, Matalevich J and Luongo C 2018 Commissioning validation of CLAS-12 torus magnet protection and cryogenic safety system *IEEE Trans. Appl. Supercond.* **28** 4703708
- [9] Wilson M N 1983 *Superconducting Magnets* (Oxford: Oxford University Press)
- [10] Cakiroglu O and Arda A 2007 Electrical properties of high temperature insulation coatings under various pressures at 298 K and 77 K *AIP Conf. Proc.* **899** p 431
- [11] Wiseman M et al 2015 Design and manufacture of the conduction cooled torus coils for the Jefferson Lab 12 GeV upgrade *IEEE Trans. Appl. Supercond.* **25** 4500505
- [12] de Hoog F R, Cozijnsen M, Yuen W Y D and Huynh H N 2004 Predicting winding stresses for wound coils of linear orthotropic material *Proc. Instrum. Mech. Eng. C* **218** 13–25
- [13] Li S and Cao J 2004 A hybrid approach for qualifying the winding process and material effects on sheet coil deformation *J. Eng. Mater. Technol.* **126** 303–13
- [14] Knight C E 1988 Residual stress and strength loss in filament-wound composites *Composite Materials: Testing and Design (8th Conf.)* ed J D Whitcomb (ASTM)
- [15] Arp V 1977 Stresses in superconducting magnets *J. Appl. Phys.* **48** 2026–36
- [16] Pojer M, Devred A and Scandale W 2006 A finite element model for mechanical analysis of LHC main dipole magnet coils *LHC Project Report 1001, Applied Superconductivity Conf. (ASC 2006)*
- [17] Fazilleau P, Ball J, Hervieu B and Pes C *CLAS 12 Solenoid Magnet Technical Design Report A-CRYOM-02-07-01-01-RT05* Centre de Saclay
- [18] Fry J R, Ruggiero G and Bergsma F 2016 Precision magnetic field mapping for CERN experiment NA62 *J. Phys. G: Nucl. Part. Phys.* **43** 125004
- [19] Ikeda T et al 1997 High-precision magnetic field mapping with a 3D Hall probe for a T-violation experiment in  $K_{\mu 3}$  decay *Nucl. Instrum. Methods Phys. Res. A* **401** 243–62
- [20] Rajput-Ghoshal R et al 2017 Field mapper for superconducting torus magnet for the Jefferson Lab 12 GeV upgrade *Int. Magnetic Measurement Workshop, IMMW-20 (Oxford, UK)*
- [21] Legg R et al 2015 Liquid nitrogen tests of a torus coil for the Jefferson Lab 12 GeV accelerator upgrade *IEEE Trans. Appl. Supercond.* **25** 4500104
- [22] Single Resistor Gain Programmable Precision Instrumentation Amplifier [www.analog.com/media/en/technical-documentation/data-sheets/1167fc.pdf](http://www.analog.com/media/en/technical-documentation/data-sheets/1167fc.pdf) pp 16–17
- [23] Designers Guide for Applying Instrument Amplifiers Effectively <http://analog.com/media/en/training-seminars/design-handbooks/designers-guide-instrument-amps-chV.pdf> pp 5–12–5–14
- [24] Compact-sized FPGA Development Platform for Prototyping Circuit Sesigns (DE0\_Nano\_User\_Manual) <http://www.terasic.com.tw/cgi-bin/page/archive.pl?Language=English&CategoryNo=139&No=593&PartNo=4>
- [25] Ekelof S 2001 The genesis of the Wheatstone bridge *Eng. Sci. Educ. J.* **10** 37–40
- [26] Lakeshore Cryotronics 2017 Cernox Temperature Sensor Technical Data [https://www.lakeshore.com/Documents/LSTC\\_appendixB\\_1.pdf](https://www.lakeshore.com/Documents/LSTC_appendixB_1.pdf) p 168
- [27] Kurt J Lesker Company 2015 Vacuum Feedthroughs: Multi-pin Bayonet Feedthrough - CF Flange, Double-Ended [www.lesker.com/newweb/feedthroughs/instrument-feedthroughs\\_mpc\\_doubleend.cfm?pgid=cf](http://www.lesker.com/newweb/feedthroughs/instrument-feedthroughs_mpc_doubleend.cfm?pgid=cf)
- [28] Kashikhin V et al 2014 Torus CLAS12-superconducting magnet quench analysis *IEEE Trans. Appl. Supercond.* **24** 4500405
- [29] National Fire Protection Association NFPA 70E—Standards for Electrical Safety in the Workplace Article-100, 110,120, 130; table 130.7(C)(9)(a) and DOE-HDBK-1092-2013 p 168
- [30] Ghoshal P K, Bachimanchi R, Fair R J, Gelhaar D, Kumar O, Philip S and Todd M 2017 Superconducting magnet power supply and hard wired quench protection at Jefferson Lab for 12 GeV upgrade *IEEE Trans. Appl. Supercond.* **27** 4703006
- [31] Pfeffer H, Flora B and Wolff D 2016 Protection of hardware: powering systems (power converter, normal-conducting, and superconducting magnets *US Particle Accelerator School (Batavia, IL)* (<https://doi.org/10.5170/CERN-2016-002.343>)
- [32] Neilsen C 2014 Hall B torus/solenoid MPS Report 502337-201 Danfysik System 8500, Model 854 Magnet Power Supply [www.danfysik.com/media/1098/model-854-datasheet.pdf](http://www.danfysik.com/media/1098/model-854-datasheet.pdf)